

Soft Wall holographic model for the minimal Composite Higgs

Domènec Espriu* and Alisa Katanaeva†

*Departament de Física Quàntica i Astrofísica and
Institut de Ciències del Cosmos (ICCUB), Universitat de Barcelona,
Martí i Franquès 1, 08028 Barcelona, Catalonia, Spain*

Abstract

We reassess employing the holographic technique to the description of 4D minimal composite Higgs model with $SO(5) \rightarrow SO(4)$ global symmetry breaking pattern. The particular 5D bottom-up holographic treatment is inspired by previous work in the context of QCD and it allows to study spin one and spin zero resonances. The resulting spectrum consists of the states transforming under the unbroken $SO(4)$ subgroup and those with quantum numbers in the $SO(5)/SO(4)$ coset. The spin one states are arranged in linear radial trajectories, and the states from the broken subgroup are generally heavier. The spin zero states from the coset space correspond to the four massless Goldstone bosons in 4D. One of them takes the role of the Higgs boson. Restrictions derived from the experimental constraints (Higgs couplings, S parameter, etc.) are then implemented and we conclude that the model is able to accommodate new vector resonances with masses in the range 2 TeV to 3 TeV without encountering phenomenological difficulties. The couplings governing the production of these new states in the processes of the SM gauge boson scattering are also estimated. The method can be extended to other breaking patterns.

* espriu@icc.ub.edu

† katanaeva@fqa.ub.edu

I. INTRODUCTION

Most of the LHC data gathered so far seems to indicate that the minimal version of the Standard Model (SM) with a doublet of complex scalar fields is compatible with the experimental results. However, many of the possible extensions involve a strongly interacting sector where perturbation theory cannot be trusted and non-perturbative methods are needed to make predictions. The extra-dimensional holographic framework is a valid option to investigate strongly coupled theories of various types and make meaningful comparisons with experiment.

The original AdS/CFT correspondence [1–3] between string theory on $AdS_5 \times S_5$ and $\mathcal{N} = 4$ super Yang–Mills gauge theory on ∂AdS_5 relates very particular theories on both sides. Here, we follow the bottom-up approach to holography – a conjectured phenomenological sprout of AdS/CFT that inherits several key concepts of the latter, but retains enough flexibility. It is also known as AdS/QCD due to being tried at and proven successful in describing several facets of the SM theory of strong interactions.

In the AdS/QCD models the spacetime is described by a five-dimensional anti-de Sitter (AdS) metric with the additional dimension labelled as z . The value $z = 0$ corresponds to the ultraviolet (UV) brane, where the theory is assumed to be described by a conformal field theory (CFT) as befits QCD at short distances. In the infrared (IR) the conformality of the metric must be broken to reproduce the confining property of QCD. This could be done either via introducing an IR brane at some finite distance in the z -direction, or making a smooth cut-off instead. The former is known as the hard wall (HW) proposal [4, 5], and the latter is called the soft wall (SW) model [6] in contrast. The SW framework is of particular phenomenological interest as it results in strongly-coupled resonances lying on linear Regge trajectories.

A viable possibility for an extended electroweak symmetry breaking sector (EWSBS) is the misaligned composite Higgs (CH) models [7]. Characteristic to these models is the breaking of the global symmetry group \mathcal{G} to a subgroup \mathcal{H} due to some non-perturbative mechanism (like condensation of the fundamental hyper-fermions constructing the Higgs and new resonances) at the scale $\Lambda_{CH} \simeq 4\pi f_{CH}$. The lightness of the Higgs is guaranteed by the identification to the Nambu–Goldstone bosons emerging after the symmetry breaking. The coset space should have capacity for at least four degrees of freedom of the Higgs doublet.

The subgroup \mathcal{H} should necessarily contain $SU(2) \times U(1)$. However, the SM gauge group itself lies in \mathcal{H}' that is rotated with respect to \mathcal{H} by a certain angle θ around one of the broken directions. Vacuum misalignment, generated by non-zero θ , is the mechanism responsible for the electroweak (EW) breaking. Furthermore, the misalignment angle θ sets the hierarchy between Λ_{CH} and the weak scale $4\pi v$. It is common to assume $v = f_{CH} \sin \theta$. One would expect $\sin \theta$ to be small but not too much, because a large scale separation may lead to a relevant amount of fine-tuning in order to keep light the states that should remain in the low energy part of the spectrum. Moreover, in order to naturally satisfy the constraint on the oblique parameter T , \mathcal{H} should accommodate the group of custodial symmetry.

The Minimal Composite Higgs Model (MCHM) of Ref. [8] provides the most economical way to incarnate these demands. It features the groups $\mathcal{G} = SO(5)$ and $\mathcal{H} = SO(4) \simeq SU(2) \times SU(2)$. Unfortunately, not much is known about the dynamics and the spectrum of this theory. The global symmetry $SO(5)$ cannot be realized with fermions at the microscopic level. Yet it is often implicitly assumed that a lot of qualitative features in CH phenomenology are similar to the ones of QCD.

There exists substantial bibliography on the application of the holographic methods in CH scenarios. One way is to construct a Randall–Sundrum model on a slice of AdS [z_{UV}, z_{IR}]. This way minimal composite Higgs scenario was realized first in Ref. [8] (and followed in Refs. [9], [10], *etc.*). The first example of the technique was proposed for the simplest case of the $SU(3) \rightarrow SU(2)$ breaking pattern in Ref. [11]. Other authors used flat 5D models with the z dimension being an orbifold S^1/Z_2 , *i.e.* restricted to a finite interval as well (see Refs. [12–14]).

The models inspired by Ref. [8] have the following characteristics. The gauge symmetry of the SM is generalized to that of $SO(5)$ and extended into the 5D bulk, where the two branes are introduced, similar to the HW option in AdS/QCD. The choice of the boundary conditions to be imposed on the 5D fields on these branes determines the symmetry breaking pattern. The Higgs is fully associated with the fifth component of the gauge field in the direction of the broken gauge symmetry (an idea first realized in Ref. [15]). An effective Higgs potential is absent at the tree-level, and its Coleman–Weinberg generation by the quantum loop corrections (dominated by the top quark contribution) breaks the EW symmetry. Emphasis is made on a way one embeds SM quarks into 5D model and their impact on the said potential; EW observables (S , T , $Z \rightarrow b\bar{b}$) are also estimated [8, 9].

CH studies have not been much elaborated in the SW framework after the initial proposal of Ref. [16]. Motivated by the much better description of QCD phenomenology that SW models provide, we would like to revisit CH models and provide an in-depth analysis of several relevant observables. We would like to put accent on the realization of the global symmetry breaking pattern and the description of spin zero fields, the fulfillment of the expected current algebra properties, such as Weinberg sum rules, and the OPE. In the present description the $SO(5) \rightarrow SO(4)$ breaking takes part in the scalar sector of the bulk Lagrangian, similarly to generalized sigma models used for QCD at long distances [17]. The Goldstone bosons are introduced explicitly, but also appear due to the gauge choice in the fifth component of the broken gauge field – that is reminiscent to what was proposed in Ref. [16]. However, quite differently from these models, the dynamics responsible for the $SO(5) \rightarrow SO(4)$ breaking is entirely “decoupled” from the SM gauge fields. In our approach, no $SO(5)$ bulk gauge symmetry is assumed for the EW sector and only strongly interacting composite states propagate in the bulk. The gauge bosons are treated in fact as external sources that do not participate in the strong dynamics (except eventually through mixing of fields with identical quantum numbers) and, hence, are entirely z -independent. We believe these premises to be well justified after what has been learned from holographic QCD over the last years. The accumulated knowledge vindicates by itself taking another look at CH models. To specify, our treatment is substantiated by the bottom-up holographic realizations of QCD given in Refs. [4–6, 18–21], but several aspects of the 5D dynamics are quite distinct for the sake of accommodating the CH physics.

As said, we concentrate on the dynamics of the strongly interacting EWSBS and its interaction with the EW sector, and no new insight into the naturalness problem or the origin of the hierarchy is provided. We also adopt the point of view that the Higgs potential, being of perturbative origin, is not the primary benefactor of the holographic analysis. For that reason we do not introduce SM fermion fields, which in CH scenarios are essential to provide the values of $\sin \theta$, Higgs mass and Higgs self-couplings among other things [22, 23].

II. HOLOGRAPHIC COMPOSITE HIGGS FRAMEWORK

A. Misalignment and operators of the strongly interacting sector

We will consider a theory where in addition to the SM \mathcal{L}_{SM} there is a new strongly interacting sector $\mathcal{L}_{str.int.}$, presumed to be conformal in the UV. A global symmetry of this sector is spontaneously broken following the pattern $\mathcal{G} \rightarrow \mathcal{H}$. There are Goldstone bosons in the coset space \mathcal{G}/\mathcal{H} , and some of them have the quantum numbers of the Higgs doublet. As the $SU(2)_L \times U(1)$ global group is necessarily included in \mathcal{H} we can couple the EW sector of the SM to the composite sector

$$\mathcal{L} = \tilde{\mathcal{L}}_{str.int.} + \mathcal{L}_{SM} + \tilde{J}_L^\alpha{}^\mu W_\mu^\alpha + \tilde{J}^Y{}^\mu B_\mu. \quad (1)$$

There only appear the conserved currents of the strongly interacting sector $J_L^\alpha{}^\mu$ and $J^Y{}^\mu$ that contain the generators of the EW group. Moreover, we have to denote the misalignment between the \mathcal{H} subgroup of the new sector and the actual \mathcal{H}' containing the W_μ^α and B_μ EW gauge bosons. In Eqn. (1) everything related to the new composite sector is marked with tildes.

Let us specify to the case of MCHM, where the global symmetry breaking pattern is $SO(5) \rightarrow SO(4)$ and there are exactly four Goldstones. We denote by T^A , $A = 1, \dots, 10$ the generators of $SO(5)$, represented by 5×5 matrices, which are traceless $\text{Tr} T^A = 0$ and normalized as $\text{Tr}(T^A T^B) = \delta^{AB}$. They separate naturally into two groups:

- The unbroken generators, in the case of MCHM those of $SO(4) \simeq SU(2)_L \times SU(2)_R$, we will call T^a , $a = 1, \dots, 6$. They are specified as

$$T_L^\alpha = \begin{pmatrix} t_L^\alpha & 0 \\ 0 & 0 \end{pmatrix}, \quad T_R^\alpha = \begin{pmatrix} t_R^\alpha & 0 \\ 0 & 0 \end{pmatrix}, \quad \alpha = 1, 2, 3, \quad (2)$$

where t_L^α , t_R^α are 4×4 matrices given by $(t_{L/R}^\alpha)_{jk} = -\frac{i}{2}(\varepsilon_{\alpha\beta\gamma}\delta_j^\beta\delta_k^\gamma \pm (\delta_j^\alpha\delta_k^4 - \delta_k^\alpha\delta_j^4))$, $j, k = 1, \dots, 4$.

- The broken generators, corresponding to the coset $SO(5)/SO(4)$, are labeled as \hat{T}^i , $i = 1, 2, 3, 4$ and defined as follows

$$\hat{T}_{IJ}^i = -\frac{i}{\sqrt{2}}(\delta_I^i\delta_J^5 - \delta_J^i\delta_I^5), \quad I, J = 1, \dots, 5. \quad (3)$$

A quantity parametrizing the vacuum misalignment and responsible for the EW symmetry breaking is the rotation angle θ that relates the linearly-realized global group $\mathcal{H} = SO(4)$ and the gauged group $\mathcal{H}' = SO(4)'$. It is natural to assign the value $\theta = 0$ to the SM, hence we denote the generators of $SO(5) \rightarrow SO(4)'$ as $\{T^a(0), \hat{T}^i(0)\}$ and those of $SO(5) \rightarrow SO(4)$ as $\{T^a(\theta), \hat{T}^i(\theta)\}$. We choose a preferred direction for the misalignment and the following connection between the generators holds

$$T^\alpha(\theta) = r(\theta)T^\alpha(0)r^{-1}(\theta), \quad \text{with } r(\theta) = \begin{pmatrix} 1_{3 \times 3} & 0 & 0 \\ 0 & \cos \theta & \sin \theta \\ 0 & -\sin \theta & \cos \theta \end{pmatrix}. \quad (4)$$

Compositeness implies that some fundamental degrees of freedom are bound together by the new “color” force (hyper-color is usually used in the CH framework). MCHM does not admit complex Dirac fermions as fundamental fields at the microscopic level due to the nature of the global “flavor” symmetry group. The anomaly-free UV complete fundamental fermion theory should have \mathcal{G} equivalent to $SU(n_1) \times \dots \times SU(n_p) \times U(1)^{p-1}$, where n_i is the number of fermions in a given irreducible representations and p counts the number of different irreps [24]. The simplest UV-completable theory will be the next-to-minimal CH with $SO(6) \rightarrow SO(5)$, featuring five Goldstone bosons (other next-to-minimal patterns are mentioned, for instance, in Ref. [25]). Nevertheless, we choose to work with MCHM because of its simplicity that serves to illustrate the general procedure.

If one chooses to avoid the particularities of the microscopic structure of the new composite states (that seems advisable on the grounds of being as general as possible), it is impossible to treat the holographic MCHM completely in the AdS/QCD fashion of Ref. [4, 6]. To some extent, due to affecting directly the operator scaling dimension Δ , the microscopic substructure sets the prescriptions for the bulk masses and UV boundary conditions, which in their turn influence all other holographic derivations. In our holographic model describing the minimal CH we only use a single entry from the list of field-operator correspondences [26]

$$A_\mu^A(x, z = \varepsilon) = 1 \cdot \phi_\mu^A(x) \leftrightarrow \mathcal{O}_\mu^A(x) \text{ with } \Delta = 3, \quad (5)$$

where $\mathcal{O}_\mu^A(x)$ are the unspecified conserved currents of the fundamental theory containing $SO(5)$ generators T^A , and $A_\mu^A(x, z)$ are dual 5D fields restricted to provide the sources $\phi_\mu^A(x)$ for the corresponding operators on the UV brane (ε is an UV regulator). We take $\Delta = 3$ (and zero bulk mass of the vector fields) as a universal feature for the conserved vector currents, because it should be so both in the case of fermionic ($\bar{\Psi}\gamma_\mu T^A \Psi$) and bosonic ($\partial_\mu s^\top T^A s$) fundamental degrees of freedom. The introduction of the scalar operator is indispensable in order to generate the breaking towards $SO(4)$. However, following a line similar to the vector case would mean inferring too much on the nature of the fundamental theory. Hence, we intend to construct the model so that this part of duality is realized in an alternative way.

The operators $\mathcal{O}_\mu^A(x)$ define the currents of Eqn. (1):

- for $A = \alpha$ (left): $\frac{g}{\sqrt{2}} \mathcal{O}_{L\mu}^\alpha(x) = g_V J_{L\mu}^\alpha$;
- for hypercharge realized as $Y = T_R^3$: $\frac{g'}{\sqrt{2}} \mathcal{O}_{R\mu}^3(x) = g_V J_\mu^Y$.

The coupling coefficients are not fully established because the operators are taken with an abstract normalization g_V that will be determined to provide agreement with the common MCHM notations. Introduction of g_V is also substantiated by the discussion of Ref. [21], where it is argued that a degree of arbitrariness in the field-operator holographic correspondence is a necessary piece of AdS/QCD constructions.

B. 5D model Lagrangian

In this subsection we put forward the details of the holographic 5D model realizing the 4D MCHM concept. We settle upon the idea that there are two composite operators, a vector and a scalar one, that define the theory, and hence we have spin one and spin zero

fields on the 5D side. These fields live in the 5D AdS bulk with a metric given by

$$g_{MN}dx^M dx^N = \frac{R^2}{z^2}(\eta_{\mu\nu}dx^\mu dx^\nu - d^2z), \quad \eta_{\mu\nu} = \text{diag}(1, -1, -1, -1). \quad (6)$$

The dynamics is governed by the following $SO(5)$ gauge invariant action

$$S_{5D} = \frac{1}{4g_5^2} \int d^5x \sqrt{-g} e^{-\Phi(z)} \text{Tr} F_{MN} F_{KL} g^{MK} g^{LN} \quad (7)$$

$$+ \frac{1}{k_s} \int d^5x \sqrt{-g} e^{-\Phi(z)} \left[\text{Tr} g^{MN} (D_M H)^\top (D_N H) - M_H^2 \text{Tr} H H^\top \right].$$

This 5D effective action includes matrix-valued scalar and vector fields and, as mentioned, is inspired by generalized sigma models used in the context of strong interactions. A similar starting action was used in the AdS/QCD study of Ref. [21]. The dimensionality of the normalization constants g_5^2 and k_s is set to compensate that of the additional dimension: $[g_5^2] = [k_s] = E^{-1}$. To have the gravitational background of a smoothly capped off AdS spacetime we introduce a SW dilaton function $\Phi(z) = \kappa^2 z^2$ in the common inverse exponent factor.

The scalar degrees of freedom are collected in the matrix-valued field H . Let us denote the group transformations $g \in SO(5)$ and $h \in SO(4)$. The matrix of the Goldstone fields ξ transforms under $SO(5)$ as: $\xi \rightarrow \xi' = g\xi h^\top$. The other scalar degrees of freedom with the quantum numbers of $SO(4)$ are collected in the matrix Σ transforming as $\Sigma \rightarrow \Sigma' = h\Sigma h^\top$. The breaking from $SO(5)$ to $SO(4)$ also appears there and is parametrized by a function $f(z)$. From these components we can construct a proper combination leading to $H \rightarrow H' = gHg^\top$

$$H = \xi \Sigma \xi^\top, \quad \Sigma = \begin{pmatrix} 0_{4 \times 4} & 0 \\ 0 & f(z) \end{pmatrix} + \sigma^a(x, z) T^a, \quad \xi = \exp \left(\frac{i\pi^i(x, z) \widehat{T}^i}{\chi_\pi} \right), \quad (8)$$

where $[\chi_\pi] = [f(z)] = E^1$. The minutiae of the scalar fields, introduced in Σ as σ^a , will be further omitted in this study. It follows then that in this representation: $H = H^\top$, the $\text{Tr} H H^\top$ quadratic piece of Eqn. (7) brings no field interactions and the value of M_H^2 is of no consequence.

Holography prescribes that every global symmetry of the 4D model comes as a gauge symmetry of its 5D dual. Thus, to make the Lagrangian invariant under the gauge transformation $A_M \rightarrow A'_M = g A_M g^{-1} + ig \partial_M g^{-1}$ the covariant derivative is introduced in the 5D action (7), defined as

$$D_M H = \partial_M H + [A_M, H], \quad D_M H \rightarrow g D_M H g^{-1}. \quad (9)$$

The field strength tensor that produces the vector field kinetic term in Eqn. (7) is

$$F_{MN} = \partial_M A_N - \partial_N A_M + [A_M, A_N]. \quad (10)$$

Generally, we take $A_M = -i A_M^A T^A$, where the upper index runs through both broken and unbroken indices $A_M^a T^a + A_M^i \widehat{T}^i$. These 5D vector fields are unrelated to the W_μ^α or B_μ gauge bosons of the EW interactions, but for their eventual mixing.

The A_μ^A fields are connected by duality to the \mathcal{O}_μ^A vector composite operators with the same generators and have the boundary condition (5). For the fifth component of the vector field we assume that

$$A_z^A(x, \varepsilon) = 0, \quad (11)$$

because there is no 4D source for it to couple to. The common holographic gauge $A_z^A \equiv 0$ fulfills this condition trivially, but this is not the only possibility. On the other hand, the dual counterpart of H and the value of M_H^2 remain unspecified. The near-boundary behavior of the Goldstone fields $\pi^i(x, z)$ will be eventually determined in Section III B from considerations of another type. The treatment of the Goldstone is an essential aspect of the model because they correspond to the four components of the Higgs doublet.

C. Extraction of 4D-relevant physics

The basic principle of AdS/CFT correspondence states that the partition function of the 4D theory and the on-shell action of its 5D holographic dual coincide in the following sense [2, 3]:

$$Z_{4D}[\phi] = \text{Exp } iS_{5D}^{on-shell} |_{\phi(x,z) \rightarrow \phi(x,z=\varepsilon)}. \quad (12)$$

Essentially, all bulk fields $\phi(x, z)$ are set to their boundary values $\phi(x, z = \varepsilon)$, which could be identified with the sources $\phi(x)$ as in the case of Eqn. (5).

The dynamics of holographic fields is governed by a set of second order equations of motion (EOMs). Thus, a 5D field can be attributed with two solutions. According to the usual AdS/CFT dogma, the leading mode at small z corresponds to the bulk-to-boundary propagator. It connects a source at the boundary and a value of a field in the bulk and should exhibit enough decreasing behavior in the IR region to render the right-hand side of Eqn. (12) finite. The subleading mode represents an infinite series of normalizable solutions, known as the Kaluza-Klein (KK) decomposition. There, the 4D and z dependencies are separated: the z -independent functions are identified with a tower of physical states at the 4D boundary that are further promoted into the bulk with the z -dependent profiles.

From consideration of the KK solutions one gets knowledge about the spectra of the composite 4D resonances. While from Eqn. (7), evaluated on the bulk-to-boundary solutions, one can extract the n -point correlation functions of the composite operators [2, 3, 27]. The 4D partition function is given by the functional integral over the fundamental fields φ contained in the selected operators (*e.g.* \mathcal{O}_μ^A) and in the fundamental Lagrangian $\mathcal{L}_{str.int.}$

$$\begin{aligned} Z_{4D}[\phi] &= \int [\mathcal{D}\varphi] \text{Exp } i \int d^4x [\mathcal{L}_{str.int.}(x) + \phi_\mu^A(x) \mathcal{O}^{A\mu}(x) + \dots] \\ &= \text{Exp} \sum_q \frac{1}{q!} \int \prod_{k=1}^q d^4x_k \langle \mathcal{O}_1(x_1) \dots \mathcal{O}_q(x_q) \rangle i\phi^1(x_1) \dots i\phi^q(x_q). \end{aligned} \quad (13)$$

From the schematic definition in Eqn. (13) and the correspondence postulate (12), it is clear that the Green functions can be obtained by the variation of the 5D effective action with respect to the sources. Diagrammatically we can represent the correlation functions by the left panel of Fig. 1, where in general the number of legs could be equal to the number n of operators in the correlator. At the same time, couplings involving the composite resonances can be estimated taking the proper term in the 5D Lagrangian, inserting the KK modes for the interacting 5D fields and integrating over the z -dimension. Due to $\ln Z_{4D} = iS_{4D}^{eff}$ a calculation of this kind brings an effective vertex.

Interaction of a given composite state with the SM gauge bosons happens through the mixing of the latter with other composite particles. Due to the misalignment the EW bosons couple to a variety of resonances, because the rotated currents \tilde{J}_μ^α overlap with different

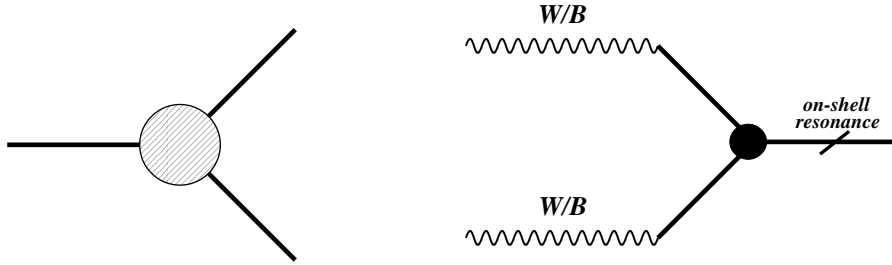


FIG. 1. Diagrams describing (left) three-point correlation function, (right) effective triple couplings between two SM gauge bosons and a composite resonance.

types of vectorial currents that are holographically connected to vector composite fields. Besides, all radial excitations in a KK tower should generally be included in the internal propagation. The procedure in this case is the following: calculate the n -point correlation function, build the effective 4D Lagrangian via attaching W_μ^α or B_μ fields as physical external sources, and reduce the legs where the composite resonances become physical and put on-shell (substituted with their KK modes). This is shown in the right panel of Fig. 1.

III. EQUATIONS OF MOTION AND THEIR SOLUTIONS

In this section we study the EOMs of the 5D fields. They are derived from the 5D action at the quadratic level

$$S_{5D}^{(2)} = \int d^5x e^{-\Phi(z)} \left\{ -\frac{1}{4g_5^2} \frac{R}{z} F_{\mu\nu}^A F^{A\mu\nu} + \frac{1}{2g_5^2} \frac{R}{z} (\partial_z A_\mu^A - \partial_\mu A_z^A)(\partial_z A^{A\mu} - \partial^\mu A_z^A) \right. \\ \left. + \frac{f^2(z)}{k_s} \frac{R^3}{z^3} \left[\left(A_\mu^i - \partial_\mu \frac{\pi^i}{\chi_\pi} \right)^2 - \left(A_z^i - \partial_z \frac{\pi^i}{\chi_\pi} \right)^2 \right] \right\}. \quad (14)$$

The sum over coincident indices is assumed for $A = \{a, i\} = 1, \dots, 10$ in the first line, and just over broken indices $i = 1, \dots, 4$ in the second. The ansatz functions are $\Phi(z) = \kappa^2 z^2$ and $f(z) \sim z$. The choice for the symmetry breaking function $f(z)$ is justified by the analyticity of the solution in the broken vector sector; the argumentation is similar to that of Ref. [21].

A. Equations of motion for the unbroken generators

In the unbroken sector with $a = 1, \dots, 6$

$$\partial_z \frac{e^{-\Phi(z)}}{z} \partial_z A_\mu^a - \frac{e^{-\Phi(z)}}{z} \square A_\mu^a - \partial_z \frac{e^{-\Phi(z)}}{z} \partial_\mu A_z^a = 0, \quad (15)$$

$$\square A_z^a = \partial^\mu \partial_z A_\mu^a. \quad (16)$$

If we act with ∂^μ on the first equation and substitute $\square A_z^a$ from the second one, we would get the third term equal to the first one. Then, the result is

$$\square \partial^\mu A_\mu^a = 0, \quad (17)$$

that implies either $\partial^\mu A_\mu^a = 0$ (transversality) or $q_{A\parallel}^2 = 0$ (longitudinal mode), where

$$A_\mu^a = A_\mu^{a\perp} + A_\mu^{a\parallel}, \quad (18)$$

with $A_\mu^{a\perp} = \mathcal{P}_{\mu\nu} A^{a\nu}$, $\mathcal{P}_{\mu\nu} = \left(\eta_{\mu\nu} - \frac{q_\mu q_\nu}{q^2}\right)$, and $A_\mu^{a\parallel} = \frac{q_\mu q_\nu}{q^2} A^{a\nu}$.

The condition (17) modifies the second equation in the system into

$$\square^2 A_z^a = 0. \quad (19)$$

While acting with \square^2 on Eqn. (15) and taking into account $q_{A\perp}^2 \neq 0$ we get the following equation for the transversal mode

$$\partial_z \frac{e^{-\Phi(z)}}{z} \partial_z A_\mu^{a\perp} - \frac{e^{-\Phi(z)}}{z} \square A_\mu^{a\perp} = 0. \quad (20)$$

However, the result for the longitudinal mode with $q_{A\parallel}^2 = 0$ turns out trivial, meaning that the remaining system for $A_\mu^{a\parallel}$ and A_z^a is underdefined. We choose to work in a class of solutions where Eqn. (19) is fulfilled with the gauge

$$A_z^a(x, z) \equiv 0. \quad (21)$$

As a result the EOM for the longitudinal mode simplifies to

$$\partial_z A_\mu^{a\parallel} = 0. \quad (22)$$

The following boundary terms are left in the on-shell action (14)

$$\frac{1}{2g_5^2} \int d^4x e^{-\Phi(z)} \frac{R}{z} A^{a\mu} (\partial_z A_\mu^a - \partial_\mu A_z^a) \Big|_\varepsilon^\infty = -\frac{1}{2g_5^2} \int d^4x \frac{R}{z} A^{a\perp\mu} \partial_z A_\mu^{a\perp} \Big|_{z=\varepsilon}. \quad (23)$$

Only the transversal term remains, giving rise to the two-point function studied in Section IV A.

Let us perform a 4D Fourier transform $A_\mu^a(x, z) = \int d^4q e^{iqx} A_\mu^a(q, z)$ and let us focus on finding solutions of the EOMs. First, the transverse bulk-to-boundary propagator, which we denote $V(q, z)$, is defined by

$$A_\mu^{a\perp}(q, z) = \phi_\mu^{a\perp}(q) \cdot V(q, z), \quad V(q, \varepsilon) = 1, \quad (24)$$

where $\phi_\mu^{a\perp}$ should be understood as a projection of the original source $\phi_\mu^{A\perp} = \mathcal{P}_{\mu\nu} \phi^{A\nu}$. The analogous longitudinal projection will be denoted by $\phi_\mu^{A\parallel}$.

From Eqn. (20), changing to the variable $y = \kappa^2 z^2$, we arrive to the following EOM

$$yV''(q, y) - yV'(q, y) + \frac{q^2}{4\kappa^2} V(q, y) = 0 \quad (25)$$

It is a particular case of the confluent hypergeometric equation (see Appendix A for a review of the properties and solutions of this equation), and the dominant mode at small z is

$$V(q, z) = \Gamma\left(-\frac{q^2}{4\kappa^2} + 1\right) \Psi\left(-\frac{q^2}{4\kappa^2}, 0; \kappa^2 z^2\right). \quad (26)$$

The subdominant solution (see Eqn. (A3)) gives us the tower of massive states, identified with vector composite resonances at the boundary. Normalizable solutions can only be found for discrete values of the 4D momentum $q^2 = M_V^2(n)$ and we may identify $V(q, z)|_{q^2=M_V^2(n)} = V_n(z)$. The KK decomposition is set as follows

$$A_\mu^{a\perp}(q, z) = \sum_{n=0}^{\infty} V_n(z) A_{\mu(n)}^{a\perp}(q). \quad (27)$$

The z profile and the spectrum can be expressed using the discrete parameter $n = 0, 1, 2, \dots$

$$V_n(z) = \kappa^2 z^2 \sqrt{\frac{g_5^2}{R}} \sqrt{\frac{2}{n+1}} L_n^1(\kappa^2 z^2), \quad M_V^2(n) = 4\kappa^2(n+1), \quad (28)$$

where $L_n^m(x)$ are the generalized Laguerre polynomials. The profiles $V_n(z)$ are subject to the Dirichlet boundary condition and are normalized to fulfill the orthogonality relation

$$\frac{R}{g_5^2} \int_0^\infty dz e^{-\kappa^2 z^2} z^{-1} V_n(z) V_k(z) = \delta_{nk}. \quad (29)$$

For the longitudinal mode, $A_\mu^{a\parallel}(q, z)$, the bulk-to-boundary solution is similarly defined. Its EOM (22), however, admits only trivial continuation into the bulk

$$A_\mu^{a\parallel}(q, z) = \phi_\mu^{a\parallel}(q) \cdot V^\parallel(q, z), \quad V^\parallel(q, z) = 1. \quad (30)$$

The previous results are well known. Let us now see the equivalent derivation in the broken sector.

B. Equations of motion for the broken generators

The EOMs for the broken sector with $i = 1, \dots, 4$ are more complicated due to the appearance of mixing with π^i

$$\partial_z \frac{e^{-\Phi(z)}}{z} (\partial_z A_\mu^i - \partial_\mu A_z^i) - \frac{e^{-\Phi(z)}}{z} \square A_\mu^i - \frac{2g_5^2 f^2(z) R^2 e^{-\Phi(z)}}{k_s z^3} \left(A_\mu^i - \frac{\partial_\mu \pi^i}{\chi_\pi} \right) = 0 \quad (31)$$

$$\frac{e^{-\Phi(z)}}{z} (\partial^\mu \partial_z A_\mu^i - \square A_z^i) - \frac{2g_5^2 f^2(z) R^2 e^{-\Phi(z)}}{k_s z^3} \left(A_z^i - \partial_z \frac{\pi^i}{\chi_\pi} \right) = 0 \quad (32)$$

$$\partial_z \frac{f^2(z) R^2 e^{-\Phi(z)}}{z^3} \left(A_z^i - \partial_z \frac{\pi^i}{\chi_\pi} \right) - \frac{f^2(z) R^2 e^{-\Phi(z)}}{z^3} \left(\partial^\mu A_\mu^i - \square \frac{\pi^i}{\chi_\pi} \right) = 0 \quad (33)$$

Combining $\partial^\mu \times$ (31) with other two equations we arrive again at the condition

$$\square \partial^\mu A_\mu^i = 0, \quad (34)$$

with the same options $\partial^\mu A_\mu^i = 0$ and $q_{A\parallel}^2 = 0$ as in the unbroken case. The condition on A_z^i is different though

$$\partial_z \frac{e^{-\Phi(z)}}{z} \square^2 A_z^i - \frac{2g_5^2 f^2(z) R^2 e^{-\Phi(z)}}{k_s z^3} \square^2 \frac{\pi^i}{\chi_\pi} = 0. \quad (35)$$

The system of equations obeyed by $A_\mu^{i\parallel}$, A_z^i and π^i is insufficient to determine them and we can only solve the problem with the help of an appropriate gauge condition. There are various possibilities, but we find the option explained below most useful for the physics we aspire to describe. We impose

$$A_z^i(x, z) = \xi \partial_z \frac{\pi^i(x, z)}{\chi}, \quad (36)$$

where the parameter ξ is arbitrary.

The fact that $\pi^i(x, z)$ appears both in the scalar part of the model Lagrangian and in this gauge condition makes it distinct from other $5D$ fields in the model. To analyze the Goldstone solution we assume that the corresponding EOM defines the z -profile $\pi(x, z)$ that couples to the physical mode $\pi^i(x)$ on the boundary. The Neumann boundary condition, $\partial_z \pi(x, z)|_{z=\varepsilon} = 0$, is imposed due to Eqn. (11).

Now both parts of Eqn. (35) have the same x -dependence, and \square^2 can be taken out of the bracket. It results in the following equation on $\pi(x, z)$

$$\partial_z \frac{e^{-\Phi(z)}}{z} \partial_z \pi(x, z) - \frac{2g_5^2 f^2(z) R^2 e^{-\Phi(z)}}{\xi k_s z^3} \pi(x, z) = 0. \quad (37)$$

At the same time it allows to get rid of A_z^i and $\partial_\mu \frac{\pi^i}{\chi_\pi}$ in Eqn. (31). Then,

$$\partial_z \frac{e^{-\Phi(z)}}{z} \partial_z A_\mu^{i\perp} - \frac{e^{-\Phi(z)}}{z} \square A_\mu^{i\perp} - \frac{2g_5^2 f^2(z) R^2 e^{-\Phi(z)}}{k_s z^3} A_\mu^{i\perp} = 0, \quad (38)$$

$$\partial_z \frac{e^{-\Phi(z)}}{z} \partial_z A_\mu^{i\parallel} - \frac{2g_5^2 f^2(z) R^2 e^{-\Phi(z)}}{k_s z^3} A_\mu^{i\parallel} = 0. \quad (39)$$

At the boundary we have the following terms in the effective $4D$ action:

$$\int d^4x \left[e^{-\Phi(z)} \frac{R}{z} \frac{1}{2g_5^2} A^{i\mu} (\partial_z A_\mu^i - \partial_\mu A_z^i) + e^{-\Phi(z)} \frac{f^2(z) R^2}{z^3} \frac{R}{k_s \chi_\pi} \left(A_z^i - \partial_z \frac{\pi^i}{\chi_\pi} \right) \right] \Big|_0^\infty \quad (40)$$

$$\xrightarrow{\xi=1} -\frac{1}{2g_5^2} \int d^4x \frac{R}{z} \left(A^{i\perp\mu} \partial_z A_\mu^{i\perp} + A^{i\parallel\mu} \partial_z A_\mu^{i\parallel} - A^{i\mu} \partial_\mu \partial_z \frac{\pi^i}{\chi_\pi} \right) \Big|_{z=\varepsilon} \quad (41)$$

The two-point function of the longitudinal mode is non-zero and that is the crucial difference from the previous sector. The choice $\xi = 1$ is explained in a minute. For now we observe that it makes identical the bulk EOMs for π^i and $A_\mu^{i\parallel}$ and eliminates the Goldstone mass term from the boundary: for $\xi = 1$ all the Goldstones (including the component associated to the Higgs) are massless. It is also instructive to justify the system of EOMs (37)–(39) by deriving them in the model where $\xi = 1$ is set from the start in Eqn. (36). That exercise is worked out in Appendix B.

As in the unbroken case we perform the $4D$ Fourier transformation and establish the propagation between the source and the bulk for the transverse solution

$$A_\mu^\perp(q, z) = \phi_\mu^{i\perp}(q) \cdot A(q, z), \quad A(q, \varepsilon) = 1. \quad (42)$$

Changing variables to $y = \kappa^2 z^2$ we arrive at the following EOM

$$yA''(q, y) - yA'(q, y) + \left(\frac{q^2}{4\kappa^2} - \frac{g_5^2(f(y)R)^2}{2yk_s} \right) A(q, y) = 0. \quad (43)$$

An analytical solution of this EOM exists either for $f^2(y) \sim y$ or $f^2(y) \sim \text{const.}$ The last option taken together with the boundary condition on $A(q, z)$ leads to the implausible conclusion: $f(y) = 0$. Therefore we turn to the linear ansatz

$$f(z) = f \cdot \kappa z, \quad (44)$$

where the constant f has the dimension of mass. We also introduce a convenient parameter

$$a = \frac{g_5^2(fR)^2}{2k_s}. \quad (45)$$

The bulk-to-boundary mode of the confluent hypergeometric equation above is specified as

$$A(q, \kappa^2 z^2) = \Gamma \left(-\frac{q^2}{4\kappa^2} + 1 + a \right) \Psi \left(-\frac{q^2}{4\kappa^2} + a, 0; \kappa^2 z^2 \right). \quad (46)$$

The other mode for discrete values of q^2 and $A(q, z)|_{q^2=M_A^2(n)} = A_n(z)$ gives the z -profiles and masses of the eigenstates

$$A_n(z) = \kappa^2 z^2 \sqrt{\frac{g_5^2}{R}} \sqrt{\frac{2}{n+1}} L_n^1(\kappa^2 z^2), \quad M_A^2(n) = 4\kappa^2 (n+1+a), \quad n = 0, 1, 2, \dots \quad (47)$$

The orthogonality relation is completely equivalent to that of Eqn. (29). In fact, the only difference is that the intercept of the Regge trajectory is larger than in the unbroken case, though the pattern is identical. These states are heavier than their unbroken counterparts just as in QCD axial vector mesons are heavier than the vector ones.

The bulk-to-boundary solution of the longitudinal EOM (39) is

$$A_\mu^{i\parallel}(q, z) = \phi_\mu^{i\parallel}(q) \cdot A^\parallel(q, z), \quad A^\parallel(q, z) = \Gamma(1+a) \Psi(a, 0; \kappa^2 z^2). \quad (48)$$

That is equivalent to the transverse propagator of Eqn. (46) but with $q^2 = 0$.

The Goldstone EOM (37) is the same as Eqn. (39). However, $\frac{1}{2}(\partial_\mu \pi^i(x))^2$ is the correct normalization of the Goldstone kinetic term in the 4D effective Lagrangian appearing after the integration over the z -dimension, and that fixes the constant factor differently

$$\pi(x, z) = F^{-1} \chi_\pi \Gamma(1+a) \Psi(a, 0; \kappa^2 z^2), \quad (49)$$

where

$$F^2 = -\frac{2R\kappa^2 a}{g_5^2} (\ln \kappa^2 \varepsilon^2 + 2\gamma_E + \psi(1+a)). \quad (50)$$

In Section IV A we will find the same F^2 in the residue of the massless pole of the broken vector correlator. The exact accordance is only possible for $\xi = 1$. Furthermore, solution (49) fixes the due boundary interaction

$$\int d^4x (-F) \partial^\mu \pi^i(x) \phi_\mu^i(x). \quad (51)$$

As a result of W_μ^α and B_μ couplings in Eqn.(1) the mixing in Eqn.(51) for $i = 1, 2, 3$ implies that the three Goldstones would be eaten by the SM gauge bosons to provide them masses proportional to F . Notice that there is no physical source to mix with the fourth Goldstone, it remains in the model as the physical Higgs particle $\pi^4(x) = h(x)$. The phenomenological discussion of its properties are postponed to a latter section.

To end the section, we introduce a convenient expression for the bulk-to-boundary propagators as the sums over the resonances (one should utilize Eqns. (A4) and (A6)):

$$V(q, z) = \sum_{n=0}^{\infty} \frac{F_V(n)V_n(z)}{-q^2 + M_V^2(n)}, \quad A(q, z) = \sum_{n=0}^{\infty} \frac{F_A(n)A_n(z)}{-q^2 + M_A^2(n)}, \quad (52)$$

$$F_A^2(n) = F_V^2(n) = \frac{8R\kappa^4}{g_5^2}(n+1). \quad (53)$$

Here $F_{V/A}(n)$ are the decay constants related to the states with the corresponding quantum numbers. The longitudinal broken and Goldstone solutions could be represented by infinite sums too.

IV. TWO-POINT CORRELATION FUNCTIONS

A. Unbroken and broken correlators

The holographic prescriptions given in Eqns. (13) and (12) allow us to define the correlation function as

$$\langle \mathcal{O}_\mu^{a/i}(q)\mathcal{O}_\nu^{b/j}(p) \rangle = \delta(p+q) \int d^4x e^{iqx} \langle \mathcal{O}_\mu^{a/i}(x)\mathcal{O}_\nu^{b/j}(0) \rangle = \frac{\delta^2 i S_{boundary}^{5D}}{\delta i \phi_\mu^{a/i}(q) \delta i \phi_\nu^{b/j}(p)}, \quad (54)$$

where the boundary remainders of the on-shell action were established in Eqns. (23) and (41). We further define the correlators

$$i \int d^4x e^{iqx} \langle \mathcal{O}_\mu^{a/i}(x)\mathcal{O}_\nu^{b/j}(0) \rangle_\perp = \delta^{ab/ij} \left(\frac{q_\mu q_\nu}{q^2} - \eta_{\mu\nu} \right) \Pi_{unbr/br}(q^2), \quad (55)$$

$$i \int d^4x e^{iqx} \langle \mathcal{O}_\mu^i(x)\mathcal{O}_\nu^j(0) \rangle_\parallel = \delta^{ij} \frac{q_\mu q_\nu}{q^2} \Pi_{br}^\parallel(q^2). \quad (56)$$

We should take into account that $\Pi_{unbr/br}(q^2)$ are subject to short distance ambiguities of the form $C_0 + C_1 q^2$ (see *e.g.* Refs. [28, 29]).

Performing the due variation in Eqn. (23) we find $\Pi_{unbr}(q^2)$ to be

$$\Pi_{unbr}(q^2) = \frac{R}{g_5^2} \left[\frac{e^{-\Phi(z)} V(q, z) \partial_z V(q, z)}{z} \right] \Big|_{z=\varepsilon}. \quad (57)$$

Let us substitute the propagator from Eqn. (26), then

$$\Pi_{unbr}(q^2) = -\frac{R}{2g_5^2} q^2 \left(\ln \kappa^2 \varepsilon^2 + 2\gamma_E + \psi \left(-\frac{q^2}{4\kappa^2} + 1 \right) \right), \quad (58)$$

where γ_E is the Euler-Mascheroni constant and ψ is the digamma function.

To separate the short distance ambiguities we perform a decomposition of the digamma function (see Eqn. (C2)) in Eqn. (58)

$$\Pi_{unbr}(q^2) = -\frac{R}{2g_5^2} (\ln \kappa^2 \varepsilon^2 + \gamma_E) q^2 - \frac{2\kappa^2 R}{g_5^2} \sum_{n=0}^{\infty} \frac{q^4}{M_V^2(n)(q^2 - M_V^2(n))}. \quad (59)$$

The first term would correspond to the ambiguity parametrizing constant C_1 , while the second one is a well convergent sum over the resonances.

An alternative procedure, introducing the resonances at an earlier stage with the use of the bulk-to-boundary propagator (52), should result in the same two-point function. Taking into account the orthogonality relation (29) we get from Eqn. (57)

$$\Pi_{unbr}(q^2) = \sum_{n=0}^{\infty} \frac{F_V^2(n)}{-q^2 + M_V^2(n)}. \quad (60)$$

The ambiguities appear as follows

$$\Pi_{unbr}(q^2) = -\frac{2\kappa^2 R}{g_5^2} \sum_n \frac{q^4}{M_V^2(n)(q^2 - M_V^2(n))} + q^2 \sum_n \frac{2\kappa^2 R/g_5^2}{M_V^2(n)} + \sum_n \frac{2\kappa^2 R}{g_5^2}. \quad (61)$$

After the proper subtractions, we are left with the first sum of Eqn. (61). This is the part relevant for the resonance description of the two-point function that coincides with the sum in Eqn. (59). Hence, the convergent correlator is

$$\hat{\Pi}_{unbr}(q^2) = \sum_{n=0}^{\infty} \frac{q^4 F_V^2(n)}{M_V^4(n)(-q^2 + M_V^2(n))}. \quad (62)$$

Concerning the subtractions, it is not surprising that they differ for the correlators derived in two different ways. It is fundamental that they are limited to the form $C_0 + C_1 q^2$, but any reordering of the manipulations may affect the results as this is a divergent and ill-defined at short distances quantity. However, it is interesting to match the two expressions of C_1 in the proportional to q^2 terms of Eqns. (61) and (59). To do that we need to introduce a regulator in the “resonance” representation – a finite number of terms in the sum, a bound at some N_{max} . Then a connection between the maximum number of resonances N_{max} and the UV regulator ε is

$$\log N_{max} = -2\gamma_E - \log \kappa^2 \varepsilon^2. \quad (63)$$

This relation is meaningful only at the leading order (*i.e.* the constant non-logarithmic part cannot be determined by this type of heuristic arguments). Finally, the last sum in Eqn. (61) behaves as $\sim N_{max}^2$ if we sum up a finite number of resonances and actually corresponds to a potentially subleading logarithmic divergence. Therefore, it can be eliminated by setting the subtraction constant C_0 .

In the broken vector sector the situation is very similar. For the transverse modes, variation of Eqn. (41) results in

$$\Pi_{br}(q^2) = \frac{R}{g_5^2} \left[\frac{e^{-\Phi(z)} A(q, z) \partial_z A(q, z)}{z} \right] \Big|_{z=\varepsilon}. \quad (64)$$

Substituting the propagator from Eqn. (46) leads to

$$\Pi_{br}(q^2) = -\frac{R}{2g_5^2}q^2 \left(1 - \frac{4\kappa^2 a}{q^2}\right) \left(\ln \kappa^2 \varepsilon^2 + 2\gamma_E + \psi\left(-\frac{q^2}{4\kappa^2} + 1 + a\right)\right). \quad (65)$$

An alternative expression for the two-point correlator is

$$\Pi_{br}(q^2) = \sum_{n=0}^{\infty} \frac{F_A^2(n)}{-q^2 + M_V^2(n)}. \quad (66)$$

And in both cases the subtraction of short distance ambiguities leads to

$$\widehat{\Pi}_{br}(q^2) = \sum_n \frac{q^4 F_A^2(n)}{M_A^4(n)(-q^2 + M_A^2(n))} - F^2, \quad (67)$$

where we find a ‘‘pion’’ pole with the ‘‘pion decay constant’’ F anticipated in Eqn. (50) and derived there from a completely different argument. It could also be expressed in the form of an infinite series

$$F^2 = \frac{2R\kappa^2 a}{g_5^2} \sum_n \frac{1}{n + 1 + a}. \quad (68)$$

Variation over the longitudinal modes in Eqn. (41) also brings this constant

$$\Pi_{br}^{\parallel}(q^2) = F^2. \quad (69)$$

Once more, fulfilling relation (63) makes an accordance between the order- q^2 subtractions. This demonstrates the ultraviolet origin of the renormalization ambiguity involved in the constant C_1 because the outcome is independent on whether we treat the broken or unbroken symmetries. The same could be implied about C_0 . Then, the determination of F^2 in (68) is straightforward as soon as we subtract the ‘‘quadratic’’ term $\sum_n \frac{2\kappa^2 R}{g_5^2}$.

In the end, these correlation functions appear in the 4D effective Lagrangian as

$$\mathcal{L}_{eff} \supset \frac{1}{2}\phi_{\mu}^a \left(\frac{q_{\mu}q_{\nu}}{q^2} - \eta_{\mu\nu}\right) \Pi_{unbr}\phi_{\nu}^a + \frac{1}{2}\phi_{\mu}^i \left(\left(\frac{q_{\mu}q_{\nu}}{q^2} - \eta_{\mu\nu}\right) \Pi_{br} + \frac{F^2 q^{\mu}q^{\nu}}{q^2}\right) \phi_{\nu}^i. \quad (70)$$

B. Vacuum polarization amplitudes of the gauge fields

We started the discussion about the holographic CH model assuming that the SM gauge fields couple to the currents of the strongly interacting sector $\widetilde{J}_{L\mu}^{\alpha}$ and $\widetilde{J}_{R\mu}^3$ as in Eqn. (1). These currents are proportional to the ones dual to the 5D fields, $\mathcal{O}_{\mu}^{a/i}$, with the EW couplings g and g' necessarily appearing. We introduced the factor g_V to modulate that proportionality. The misalignment should also be taken into account. In the notation of Eqn. (4), a rotated operator can be given in terms of the original ones as ($\alpha, i = 1, 2, 3$ here)

$$\widetilde{\mathcal{O}}_{L/R\mu}^{\alpha} = \frac{1 \pm \cos \theta}{2} \mathcal{O}_{L\mu}^{\alpha} + \frac{1 \mp \cos \theta}{2} \mathcal{O}_{R\mu}^{\alpha} \mp \frac{\sin \theta}{\sqrt{2}} \mathcal{O}_{\mu}^i. \quad (71)$$

The two-point correlators of physical interest are

$$i \int d^4x e^{iqx} \langle \tilde{J}_{L\mu}^\alpha(x) \tilde{J}_{L\nu}^\beta(0) \rangle = \delta^{\alpha\beta} \frac{g^2}{2} \left[\left(\frac{q_\mu q_\nu}{q^2} - \eta_{\mu\nu} \right) \Pi_{LL}(q^2) + \frac{q_\mu q_\nu}{q^2} \Pi_{LL}^\parallel(q^2) \right], \quad (72)$$

$$i \int d^4x e^{iqx} \langle \tilde{J}_{R\mu}^\alpha(x) \tilde{J}_{R\nu}^\beta(0) \rangle = \delta^{\alpha\beta} \frac{g'^2}{2} \left[\left(\frac{q_\mu q_\nu}{q^2} - \eta_{\mu\nu} \right) \Pi_{RR}(q^2) + \frac{q_\mu q_\nu}{q^2} \Pi_{RR}^\parallel(q^2) \right], \quad (73)$$

$$2i \int d^4x e^{iqx} \langle \tilde{J}_{L\mu}^\alpha(x) \tilde{J}_{R\nu}^\beta(0) \rangle = \delta^{\alpha\beta} \frac{gg'}{2} \left[\left(\frac{q_\mu q_\nu}{q^2} - \eta_{\mu\nu} \right) \Pi_{LR}(q^2) + \frac{q_\mu q_\nu}{q^2} \Pi_{LR}^\parallel(q^2) \right]; \quad (74)$$

where we defined the quantities

$$\Pi_{diag}(q^2) = \Pi_{LL}(q^2) = \Pi_{RR}(q^2) = \frac{1 + \cos^2 \theta}{2g_V^2} \Pi_{unbr}(q^2) + \frac{\sin^2 \theta}{2g_V^2} \Pi_{br}(q^2), \quad (75)$$

$$\Pi_{LR}(q^2) = \frac{\sin^2 \theta}{g_V^2} (\Pi_{unbr}(q^2) - \Pi_{br}(q^2)), \quad (76)$$

$$\Pi_{LL}^\parallel(q^2) = \Pi_{RR}^\parallel(q^2) = \frac{\sin^2 \theta}{2g_V^2} F^2, \quad \Pi_{LR}^\parallel(q^2) = -\frac{\sin^2 \theta}{g_V^2} F^2. \quad (77)$$

The relevant quadratic contribution of the gauge bosons to the 4D partition function is

$$\begin{aligned} \mathcal{L}_{eff} \supset & \left(\frac{q^\mu q^\nu}{q^2} - \eta^{\mu\nu} \right) \frac{1}{4} \Pi_{diag}(q^2) (g^2 W_\mu^\alpha W_\nu^\alpha + g'^2 B_\mu B_\nu) \\ & + \frac{F^2 \sin^2 \theta}{8g_V^2} \frac{q^\mu q^\nu}{q^2} (g^2 W_\mu^\alpha W_\nu^\alpha + g'^2 B_\mu B_\nu) \\ & + \left(\frac{q^\mu q^\nu}{q^2} - \eta^{\mu\nu} \right) \frac{1}{4} \Pi_{LR}(q^2) g g' W_\mu^3 B_\nu - \frac{q^\mu q^\nu}{q^2} \frac{F^2 \sin^2 \theta}{4g_V^2} g g' W_\mu^3 B_\nu. \end{aligned} \quad (78)$$

The mass terms in the effective Lagrangian can be determined from the lowest order in q^2 . Both for the longitudinal and transverse W and Z gauge bosons we get

$$M_W^2 = \frac{g^2 \sin^2 \theta}{4 g_V^2} F^2, \quad M_Z^2 = \frac{g^2 + g'^2 \sin^2 \theta}{4 g_V^2} F^2, \quad (79)$$

while the photon stays massless.

C. Left–right correlator and sum rules

The vacuum polarization amplitudes receive contributions from the new physics (new massive resonances in the loops). To quantify deviations with respect to SM, the EW “oblique” precision parameters were introduced [30, 31]. The most relevant for the discussion of the CH models are the S and T parameters of Peskin and Takeuchi [31]. As we already mentioned, a particular feature of MCHM is that due to the custodial symmetry of the strongly interacting sector the tree-level correction to the T parameter vanishes. Bearing in mind that the holographic description is meant to be valid only in the large N_{hc} limit, loop corrections are not easily tractable. Thus, we focus on the S parameter connected to the $\Pi_{LR}(q^2)$ as follows

$$S = -4\pi \Pi'_{LR}(0) = \frac{2\pi R \sin^2 \theta}{g_5^2 g_V^2} [\gamma_E + \psi(1+a) + a\psi_1(1+a)]. \quad (80)$$

Alternatively, it could be expressed through masses and decay constants:

$$S = 4\pi \frac{\sin^2 \theta}{g_V^2} \left[\sum_n \frac{F_V^2(n)}{M_V^4(n)} - \sum_n \frac{F_A^2(n)}{M_A^4(n)} \right]. \quad (81)$$

The experimental bounds on the S parameter are essential for the numerical analysis of Section VI.

Further, we would like to investigate the validity of the equivalent of the Weinberg sum rules (WSR) that relate the imaginary part of $\Pi_{LR}(q^2)$ to masses and decay constants of vector resonances in the broken and unbroken channels, respectively. We start with the subtracted correlators $\widehat{\Pi}_{unbr}$ and $\widehat{\Pi}_{br}$ of Eqns. (62) and (67), then select a suitable integration circuit and formally obtain

$$\frac{1}{\pi} \int_0^\infty \frac{dt}{t} \text{Im} \Pi_{unbr}(t) = \sum_n \frac{F_V^2(n)}{M_V^2(n)}, \quad (82)$$

$$\frac{1}{\pi} \int_0^\infty \frac{dt}{t} \text{Im} \Pi_{br}(t) = \sum_n \frac{F_A^2(n)}{M_A^2(n)} + F^2. \quad (83)$$

However, these expressions are ill-defined: the external contour does not vanish, and the imaginary part of the poles should have been specified. The latter can be done following Vainshtein, *i.e.* replacing $M_V^2(n)$ in Eqn. (62) with $M_V^2(n)(1 - i\epsilon)$. This prescription reproduces the correct residues. Additionally, the left hand sides are generically divergent while the sum over resonances possesses an essential singularity on the real axis when the number of resonances N_{max} encircled in the contour tends to infinity.

We expect to see the convergence properties of the integrals on the left hand side of (82) and (83) improved when they are gathered in the left-right combination. For the uniformity of notation we introduce the sum $F^2 = \sum_{n < N_{max}} F^2(n)$ (from Eqn. (68)). Then,

$$\frac{1}{\pi} \int_0^{M^2(N_{max})} \frac{dt}{t} \text{Im} \Pi_{LR}(t) = \frac{\sin^2 \theta}{g_V^2} \sum_{n < N_{max}} \left(\frac{F_V^2(n)}{M_V^2(n)} - \frac{F_A^2(n)}{M_A^2(n)} - F^2(n) \right). \quad (84)$$

In QCD Π_{LR} decays fast enough so that the external contour contribution is negligible when enough resonances are encircled, and this integral vanishes. The equality of Eqn. (84) to zero is the first WSR for QCD, and the same arguments allow one to derive the second WSR

$$\frac{1}{\pi} \int_0^{M^2(N_{max})} dt \text{Im} \Pi_{LR}(t) = \frac{\sin^2 \theta}{g_V^2} \sum_{n < N_{max}} (F_V^2(n) - F_A^2(n)) = 0. \quad (85)$$

In fact, it is well known that in QCD including just the first resonances in the sum provides a fair agreement with phenomenology [32]. In any case, the convergence of the dispersion relation (no subtraction is needed) indicates that the limit $N_{max} \rightarrow \infty$ could be taken in QCD.

To understand whether the situation is indeed analogous to QCD we should address these two questions: (a) can the contour integral be neglected? (b) if so, is the integral on the left hand side converging?

To answer the first question we consider $\Pi_{LR}(Q^2)$, given explicitly in Eqn. (C1) with Euclidean momenta $Q^2 = -q^2$, and expand it for large Q^2 (we make use of the Stirling's expansion of the ψ function)

$$\frac{g_V^2 \Pi_{LR}(Q^2)}{Q^2} = \sin^2 \theta \frac{2\kappa^2 a R}{Q^2 g_5^2} \left(\ln \frac{Q^2}{4\kappa^2} + \ln \kappa^2 \varepsilon^2 - \frac{2\kappa^2 a}{Q^2} \right) + \mathcal{O} \left(\frac{1}{Q^6} \right). \quad (86)$$

This limit is constrained to the (unphysical) region of $|\arg Q^2| < \pi$, while the value on the physical axis ($0 < \text{Re } q^2 = -\text{Re } Q^2$) stays ill-defined (needs a prescription, such as the one discussed above). However, we are now in position to discuss the convergence of the outer part of the circuit in Eqns. (84) and (85). Due to the presence of the $\ln Q^2/Q^2$ and $1/Q^2$ terms the correlator does not vanish fast enough to make the issue similar to the QCD case. Therefore, the corresponding dispersion relation requires one subtraction constant c to parametrize the part of $\Pi_{LR}(Q^2)$ not determined by its imaginary component

$$\frac{\Pi_{LR}(Q^2)}{Q^2} = \int_0^\infty \frac{dt}{t + Q^2 - i\epsilon} \frac{1}{\pi} \frac{\text{Im} \Pi_{LR}(t)}{t} + c. \quad (87)$$

In the deep Euclidean region one could use an expansion

$$\frac{1}{t + Q^2} = \frac{1}{Q^2} - \frac{1}{Q^2} t \frac{1}{Q^2} + \dots \quad (88)$$

and then the dispersion relation in the large Q^2 limit looks as

$$\frac{\Pi_{LR}(Q^2)}{Q^2} = c + \frac{1}{Q^2} \frac{1}{\pi} \int_0^\infty \frac{dt}{t} \text{Im} \Pi_{LR}(t) - \frac{1}{Q^4} \frac{1}{\pi} \int_0^\infty dt \text{Im} \Pi_{LR}(t) + \dots \quad (89)$$

The next step is to encircle a large, but finite, number of resonances. That is, we take $N_{max} < \infty$ connected to the UV cut-off via the relation (63). The dispersion relation still holds and Eqn. (89) can be compared order by order with the large Q^2 expansion given in Appendix C. Holding to the assumptions made there, we obtain

$$\int_0^{M^2(N_{max})} \frac{dt}{t} \text{Im} \Pi_{LR}(t) = 0, \quad (90)$$

that establishes the formal validity of the first WSR

$$\sum_{n < N_{max}} \left(\frac{F_V^2(n)}{M_V^2(n)} - \frac{F_A^2(n)}{M_A^2(n)} - F^2(n) \right) = 0. \quad (91)$$

We further stress that the situation is rather unsimilar to the one of real QCD, essentially because F^2 is logarithmically dependent on the cut-off. On the other hand, the situation in the holographic CH scenario is quite analogous to the holographic QCD model of Ref. [21].

We just proved that the sum over vector resonances $\sum_{n < N_{max}} \left(\frac{F_V^2(n)}{M_V^2(n)} - \frac{F_A^2(n)}{M_A^2(n)} \right)$ is itself cut-off dependent for $N_{max} \rightarrow \infty$. This implies that symmetry restoration takes place very slowly in the UV and saturation with the ground state resonance is questionable both in holographic CH and holographic QCD. It seems fair to conclude that these peculiarities represent a pitfall of holography rather than a characteristic of the CH model.

Finally, the nullification of the $\frac{1}{Q^4}$ term in (C6) leads to

$$\frac{1}{\pi} \int_0^{M^2(N_{max})} dt \text{Im} \Pi_{LR}(t) = 0, \quad (92)$$

that formally proves the second WSR of Eqn. (85). Again, a cut-off should be imposed to guarantee convergence of both the integral of the imaginary part over the real axis and of the sum over resonances.

V. HIGHER ORDER CORRELATORS AND COUPLINGS

Let us write down several 5D interactions of phenomenological interest. At the three-point level they are

$$S_{5D}^{(3)} \supset i \frac{R}{g_5^2} \int d^5 x e^{-\kappa^2 z^2} z^{-1} \left(\partial_\mu A_\nu^A A^{B\mu} A^{C\nu} \text{Tr} T^A [T^B, T^C] - \partial_z A_\mu^A A_z^i A^{B\mu} \text{Tr} T^A [T^i, T^B] \right. \\ \left. + \partial_\mu A_z^i A_z^j A^{A\mu} \text{Tr} T^i [T^j, T^A] \right) + (fR)^2 \kappa^2 \frac{R}{k_s} \int d^5 x e^{-\kappa^2 z^2} z^{-1} \frac{h}{\chi_\pi} (A_L - A_R)_\mu^\alpha A_{br}^{\alpha\mu}. \quad (93)$$

To prevent misunderstanding we specify the left, right or broken origin of vector field $A_\mu(x, z)$ where it is needed (they go with $\alpha = 1, 2, 3$). Otherwise, the fields with $i, j = 1, 2, 3, 4$ are from the broken sector, and $A, B, C = 1, \dots, 10$ ones encompass all options. The fourth Goldstone field $\pi^4(x, z)$ is denoted as $h(x, z)$ henceforth. At the four-point level we have

$$S_{5D}^{(4)} \supset \frac{R}{4g_5^2} \int d^5 x e^{-\kappa^2 z^2} z^{-1} \left(A_\mu^A A_\nu^B A^{C\mu} A^{D\nu} \text{Tr} [T^A, T^B] [T^C, T^D] - 2A_z^i A_\mu^A A_z^j A^{B\mu} \text{Tr} [T^i, T^A] [T^j, T^B] \right) \\ + (fR)^2 \kappa^2 \frac{R}{4k_s} \int d^5 x \frac{e^{-\kappa^2 z^2}}{z} \frac{h^2}{\chi_\pi^2} \left((A_{L\mu}^\alpha - A_{R\mu}^\alpha)^2 - 2A_{br\mu}^{\alpha 2} \right). \quad (94)$$

The commutators there can be simplified with the Lie algebra of $SO(5)$

$$[T_L^\alpha, T_L^\beta] = i\varepsilon^{\alpha\beta\delta} T_L^\delta, \quad [T_R^\alpha, T_R^\beta] = i\varepsilon^{\alpha\beta\delta} T_R^\delta, \quad [T_L^\alpha, T_R^\beta] = 0, \quad \alpha, \beta, \delta = 1, 2, 3 \\ [T^a, \hat{T}^i] = \hat{T}^j (t^a)^{ji}, \quad [\hat{T}^i, \hat{T}^j] = (t_a)^{ji} T^a, \quad a = 1, \dots, 6, \quad i = 1, \dots, 4.$$

Here $t^a = \{t_L^\alpha, t_R^\alpha\}$, see the definition after Eqn. (2).

The expressions for $S_{5D}^{(3)}$ and $S_{5D}^{(4)}$ are already simplified with the gauge choice $A_z^a = 0$ in the unbroken channel. The Higgs-related terms proportional to $(fR)^2$ come from the square of the covariant derivative in Eqn. (7). Taking into account that in the broken sector imposed with $\xi = 1$ we had $A_z^i = \frac{\partial_z \pi^i}{\chi_\pi}$, we reveal the following interactions involving the Higgs from the F_{MN}^2 term

$$\frac{R}{2g_5^2} \int d^5 x \frac{e^{-\kappa^2 z^2}}{z} \left[\frac{\partial_z h}{\chi_\pi} (A_L - A_R)_\mu^\alpha \partial_z A_{br}^{\alpha\mu} + \frac{1}{4} \left(\frac{\partial_z h}{\chi_\pi} \right)^2 \left((A_{L\mu}^\alpha - A_{R\mu}^\alpha)^2 + A_{br\mu}^{\alpha 2} \right) \right]. \quad (95)$$

We are interested in triple and quartic couplings between the Higgs boson and the SM gauge bosons. In the standard MCHM picture these interactions have a given parametrization in the coordinate space

$$g_{hWW}^{SM} \cos \theta W_\mu^+ W^{-\mu} h + g_{hZZ}^{SM} \cos \frac{\theta}{2} Z_\mu Z^\mu h + \frac{\cos 2\theta}{4} \left(g^2 W_\mu^+ W^{-\mu} + \frac{g^2 + g'^2}{2} Z_\mu Z^\mu \right) hh, \quad (96)$$

$$g_{hWW}^{SM} = gM_W, \quad g_{hZZ}^{SM} = \sqrt{g^2 + g'^2} M_Z, \quad (97)$$

with $W_\mu^\pm = \frac{W_\mu^1 \mp i W_\mu^2}{\sqrt{2}}$, $Z_\mu = \frac{1}{\sqrt{g^2 + g'^2}} (g W_\mu^3 - g' B_\mu)$.

In our 5D model the effective couplings for hWW and $hhWW$ originate from

$$\mathcal{L}_{eff} \supset i \frac{g^2}{4g_V^2} h(q) W^{\alpha\ \mu}(k_1) W^{\beta\ \nu}(k_2) \langle h(q) | \tilde{\mathcal{O}}_{L\mu}^\alpha(k_1) \tilde{\mathcal{O}}_{L\nu}^\beta(k_2) | 0 \rangle \quad (98)$$

$$+ i \frac{g^2}{4g_V^2} h(q_1) h(q_2) W^{\alpha\ \mu}(k_1) W^{\beta\ \nu}(k_2) \langle h(q_1) h(q_2) | \tilde{\mathcal{O}}_{L\mu}^\alpha(k_1) \tilde{\mathcal{O}}_{L\nu}^\beta(k_2) | 0 \rangle. \quad (99)$$

Z boson couplings can be taken into consideration after addition of the terms generated by $\tilde{\mathcal{O}}_{L\mu}^3 \tilde{\mathcal{O}}_{R\nu}^3$, $\tilde{\mathcal{O}}_{R\mu}^3 \tilde{\mathcal{O}}_{L\nu}^3$ and $\tilde{\mathcal{O}}_{R\mu}^3 \tilde{\mathcal{O}}_{R\nu}^3$ operator combinations. Their derivation follows closely that of the W^+W^- , so we just include them in the final result.

Particularities of calculating the matrix elements in (98) and (99) can be found in Appendix D. The couplings to the EW gauge bosons appear in the effective Lagrangian as

$$\mathcal{L}_{eff} \supset \frac{g_{hWW}^{SM} \cos \theta}{\sqrt{2} g_V} \cdot \frac{1}{2} (W^{+\mu}(k_2) W_\mu^-(k_1) + W^{-\mu}(k_2) W_\mu^+(k_1)) h(q) \quad (100)$$

$$+ \frac{g^2 \cos 2\theta}{8g_V^2} \cdot \frac{1}{2} (W_\mu^+(k_1) W^{-\mu}(k_2) + W_\mu^-(k_1) W^{+\mu}(k_2)) h(q_1) h(q_2) \quad (101)$$

$$+ \frac{g_{hZZ}^{SM} \cos \theta}{\sqrt{2} g_V} \cdot \frac{1}{2} Z^\mu(k_2) Z_\mu(k_1) h(q) \quad (102)$$

$$+ \frac{(g^2 + g'^2) \cos 2\theta}{8g_V^2} \cdot \frac{1}{2} Z_\mu(k_1) Z^\mu(k_2) h(q_1) h(q_2), \quad (103)$$

$$g_{hWW}^{SM} = \frac{g^2 F \sin \theta}{2g_V}, \quad g_{hZZ}^{SM} = \frac{(g^2 + g'^2) F \sin \theta}{2g_V}, \quad (104)$$

where the factors in the last line indeed correspond to the SM notation of Eqn. (97) due to the definition of masses in Eqn. (79). The only thing missing to have the exact MCHM factors of Eqn. (96) is the proper choice of the so far free parameter

$$g_V = \frac{1}{\sqrt{2}}. \quad (105)$$

Note, that this value is obtained in the approximation $M_W^2 \ll 4\kappa^2$ assumed in the calculations of Appendix D.

Let us now turn to the part of Eqn. (93) independent of A_z and Higgs modes

$$i \frac{R}{g_5^2} \int d^5 x e^{-\kappa^2 z^2} z^{-1} \partial_\mu A_\nu^A A^{B\mu} A^{C\nu} \text{Tr} T^A [T^B, T^C] \quad (106)$$

The commutator is proportional to the epsilon-tensor if none of the three fields is A_{br}^4 . In the opposite case we rather obtain a Kronecker delta.

There is an interaction between three vector 5D fields in Eqn. (106). In order to procure a coupling of a vector resonance to two EW gauge bosons one of the fields should be taken in its KK representation, while the other two should be given by their bulk-to-boundary propagators coupled later to the corresponding gauge field sources. The details of these calculations are presented in Appendix E.

We limit ourselves to listing just the interactions for the ground states of the composite resonances

$$\begin{aligned} \mathcal{L}_{eff} \supset & \frac{1}{2} W_{\mu_2}^\alpha(q_2) W_{\mu_3}^\beta(q_3) \text{Lor}^{\mu_1\mu_2\mu_3}(q_1, q_2, q_3) (-i\varepsilon^{\alpha\beta\delta}) \\ & \times (A_{\mu_1}^{L\delta}(q_1) g_{LWW} + A_{\mu_1}^{R\delta}(q_1) g_{RWW} - A_{\mu_1}^{Br\delta}(q_1) g_{BrWW}) \end{aligned} \quad (107)$$

$$+ W_{\mu_2}^\alpha(q_2) B_{\mu_3}(q_3) \text{Lor}^{\mu_1\mu_2\mu_3}(q_1, q_2, q_3) (-i\varepsilon^{\alpha\beta\delta}) \quad (108)$$

$$\times (A_{\mu_1}^{L\delta}(q_1) g_{LWB} + A_{\mu_1}^{R\delta}(q_1) g_{RWB}), \quad (109)$$

where the notation $\text{Lor}^{\mu_1\mu_2\mu_3}(q_1, q_2, q_3)$ was given in Appendix E, and we introduced

$$g_{L/RWW} = \frac{g^2}{4g_V^2} \sqrt{\frac{R}{2g_5^2}} [1 \pm \cos\theta + a \sin^2\theta (a\psi_1(1+a) - 1)], \quad (110)$$

$$g_{BrWW} = \frac{g^2}{4g_V^2} \sqrt{\frac{R}{g_5^2}} \frac{\sin\theta}{1+a}, \quad (111)$$

$$g_{LWB} = g_{RWB} = \frac{gg'}{4g_V^2} \sqrt{\frac{R}{2g_5^2}} a \sin^2\theta [1 - a\psi_1(1+a)]. \quad (112)$$

The numerical values of these couplings will be estimated in the next section.

VI. NUMERICAL RESULTS FOR MASSES AND COUPLINGS

A very stringent limit on any new physics contribution comes from the experimental bounds on the S parameter, calculated using 5D techniques in Eqn. (80) or (81). Recent EW precision data (see Ref. [33]) constraints it to the region

$$S = -0.01 \pm 0.10. \quad (113)$$

There are three a priori free parameters in our expression for S : $\sin\theta$, a and $\frac{R}{g_5^2}$; and g_V is assumed to be fixed as in Eqn. (105). a is related to the symmetry breaking by $f(z)$: at $a = 0$ there is no breaking, the unbroken and broken vector modes have the same mass. In principle, $\frac{R}{g_5^2}$ could be evaluated by comparing holographic two-point function to the perturbative calculation of the Feynman diagram (*e.g.*, of a hyper-fermion loop) at the leading order in large Q^2 momenta, as it is usually done in the holographic realizations of QCD. As we would expect to get the hyper-color trace in the loop, it could be estimated that there is a proportionality $\frac{R}{g_5^2} \propto N_{hc}^p$ (power p depends on the particular representation). However, we deliberately made no hypothesis on the fundamental substructure, and could only expect that very large values of $\frac{R}{g_5^2}$ correspond to the large- N_{hc} limit. To have an idea of the scale of this quantity, we recall that for $N_c = 3$ QCD one has $\frac{R}{g_5^2} \sim 0.3$ [21].

We present the effect of the current S -constraint on the $(\sin\theta, a, R/g_5^2)$ plane in Fig. 2. The larger the value of $\sin\theta$ the smaller the allowed region for a and R/g_5^2 . We only consider $\sin\theta \leq 0.34$ due to the present bounds on the misalignment in MCHM [34] (for the the SM fermions in the spinorial representation of $SO(5)$). That bound is valid under the assumption that the coupling of the Higgs to gauge bosons is $\kappa_V = \sqrt{1 - \sin^2\theta}$, and it was demonstrated in Section V that this is the case of our holographic model too. Otherwise, we can take a more model-independent estimation from the latest ATLAS and CMS combined measurements with the LHC Run 1 dataset [33] that lead to $\kappa_V = 1.04 \pm 0.05$ at one standard deviation. Taken at two standard deviations it results once again in $\sin\theta \leq 0.34$. Nevertheless, stricter

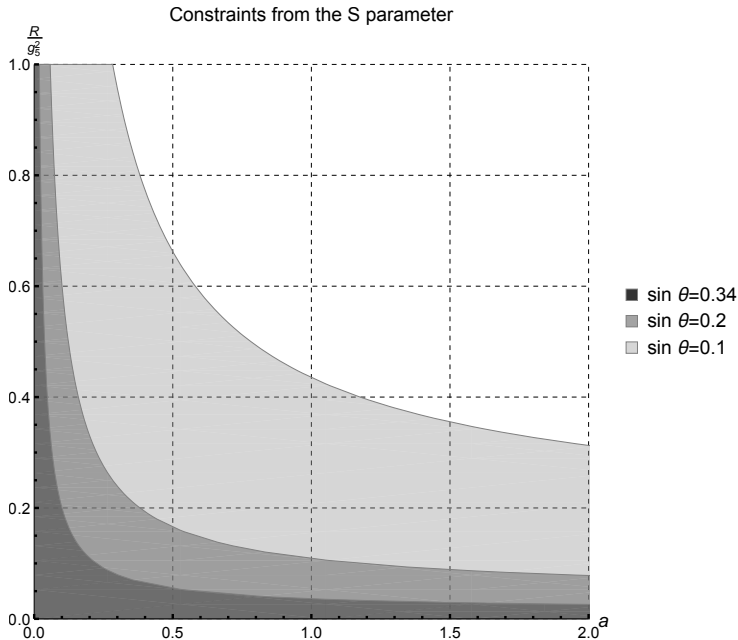


FIG. 2. The $(\sin \theta, a, R/g_5^2)$ parameter region allowed by the S parameter restraints.

(lower) bounds could also be encountered in the literature (Run 2 analyses [35, 36], for instance).

No information on the mass scale κ could be retrieved from the EW precision data. However, we can relate it to the low-energy observables through the definition of the W boson mass in Eqn. (79). It is connected to the EWSB scale $v = 246$ GeV and we can equate

$$M_W^2 = \frac{g^2 v^2}{4} = \frac{g^2 F^2 \sin^2 \theta}{4g_V^2}. \quad (114)$$

With F given in Eqn. (50), the following condition on κ is valid:

$$\frac{g_V^2 v^2}{\sin^2 \theta} + \frac{2\kappa^2 R}{g_5^2} a (\ln \kappa^2 \varepsilon^2 + 2\gamma_E + \psi(1+a)) = 0. \quad (115)$$

Let us further set

$$\varepsilon = \frac{1}{\Lambda_{\text{cut-off}}} \simeq \frac{1}{4\pi f_{CH}} = \frac{\sin \theta}{4\pi v}. \quad (116)$$

Here $\Lambda_{\text{cut-off}} = \Lambda_{CH} \simeq 4\pi f_{CH}$ is the range of validity of the effective theory of the composite resonances, which could be postulated as a natural cut-off in the present bottom-up model. We can also rework the connection between the number of resonances cut-off N_{max} and ε :

$$N_{max} = 16\pi^2 \frac{v^2}{\kappa^2 \sin^2 \theta} e^{-2\gamma_E}. \quad (117)$$

Setting $g_V = \frac{1}{\sqrt{2}}$, we collect the results in Table I. There, we substitute the estimation of κ with that of the characteristic mass $M_* = \sqrt{4\kappa^2}$, equal to the mass of the ground vector state – the lightest massive state in our spectrum. We take the values of a saturating the S -bound, thus, these are the minimal estimations for M_* . Should it be found that S is p

TABLE I. Different predictions of the minimal vector masses for $\sin \theta = 0.1, 0.2$ and 0.34 .

$\sin \theta$	$\frac{R}{g_5^2}$	a	$M_* = M_V(0), \text{ TeV}$	$M_A(0), \text{ TeV}$	$\sim N_{max}$
0.1	0.1	266.3	0.22	3.68	> 20 k
0.1	0.3	2.212	1.28	2.29	740
0.1	1	0.283	1.88	2.13	340
0.1	10	0.022	2.10	2.12	270
0.2	0.1	1.176	1.79	2.64	93
0.2	0.3	0.225	2.28	2.52	58
0.2	1	0.058	2.43	2.50	50
0.2	10	0.006	2.49	2.50	48
0.34	0.1	0.225	2.84	3.14	12
0.34	0.3	0.065	3.00	3.09	11
0.34	1	0.019	3.05	3.08	10
0.34	10	0.002	3.07	3.08	10

times smaller, our evaluations for M_* become roughly p times larger. For a given set of $\frac{R}{g_5^2}$ and $\sin \theta$ lower values of a are permitted and result in larger M_* . In addition, larger a leads to larger splitting between vector fields aligned in different (unbroken and broken) directions. It is evident from Table I that the splitting almost disappears starting from $\frac{R}{g_5^2} = 10$ for the demonstrated values of $\sin \theta$. We also notice that the effective “ N_{hc} -infinity” is heralded by the degenerate vector masses in the unbroken and broken sectors and starts rather early because $\frac{R}{g_5^2} = 10$ fit brings similar results to, say, $\frac{R}{g_5^2} = 1000$. It is an interesting observation, because in the original AdS/CFT conjecture the strongly coupled Yang–Mills theory on the 4D side of the correspondence should be in the limit $N_c \gg 1$. Of course, in phenomenological AdS/QCD models the duality is commonly extended for the finite values of N_c , so we take into consideration a set of smaller $\frac{R}{g_5^2}$ as well.

In Fig. 3 we depict a broader range of M_* values. The dependencies on the model parameters could be easily traced from there. In the parameter space $(\sin \theta, a, \frac{R}{g_5^2})$ we can fix any two values, then the growth of the third parameter results in lower M_* (as long as it does not appear in the prohibited zone). Pursuing higher degree of breaking a results in unlikely small masses in the areas that are not well-restrained by the S parameter. We speak of masses below 2 TeV at smaller values of $\frac{R}{g_5^2}$ and $\sin \theta$. Higher values of other two parameters are more efficiently cut off by the S bound. In general, 2.0 – 4.0 TeV states are expected. We also recollect that in a tower of resonances of one type we have a square root growth with the number of a resonance. Thus, for a lowish value of M_* there is a tower with several comparatively low-lying states. For instance, for the input set $(\sin \theta, a, R/g_5^2) = (0.1, 2.2, 0.3)$ we have $M_* = 1.3$ TeV and the tower masses are $M_V(n) = \{1.3, 1.8, 2.3, 2.6, \dots\}$ TeV.

In Fig. 4 we present the numerical analysis resulting from Eqns. (110), (111) and (112), showing the possible values of the couplings between the left, right and broken resonances and a W^+W^- or W^3B -pair. It is clear that the left resonances couple more strongly than the right ones thanks to the dampening the latter get with $\cos \theta$ being rather close to 1. All the WW couplings exhibit a logarithmic growth with $\frac{R}{g_5^2}$. The parameter a was taken to be saturating the S -bound of Fig. 2 and is rendered quite close to zero at higher values of R/g_5^2

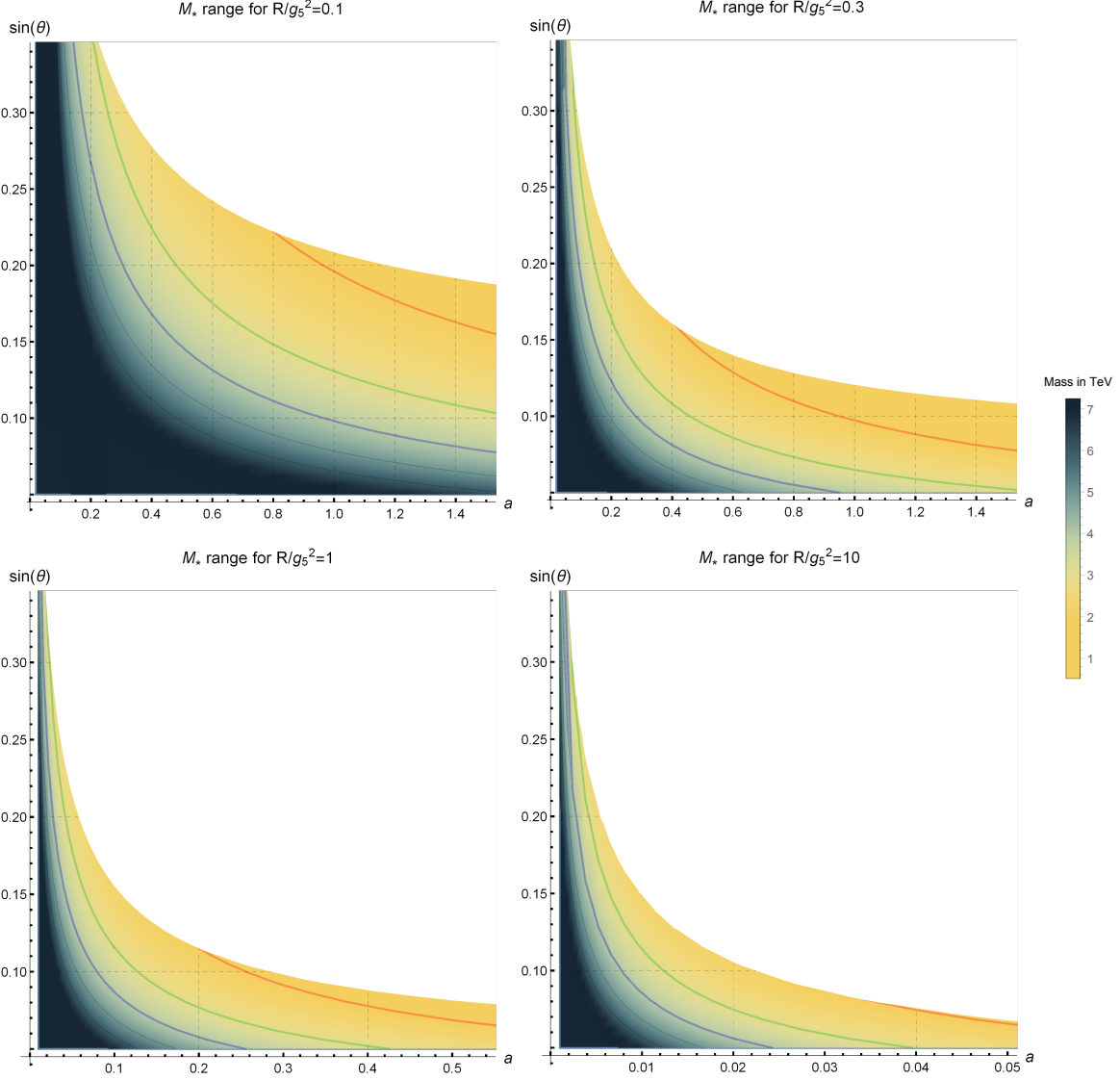


FIG. 3. The density plots of M_* for different values of R/g_5^2 . The colored curves represent the lines of constant M_* : the red one – $M_* = 2$ TeV, the green one – $M_* = 3$ TeV, the blue one – $M_* = 4$ TeV and successive black curves for higher integer values. The white area represents the sector prohibited by the S bound.

especially for larger $\sin \theta$. The coupling including the B meson is rather small in comparison to the WW ones due to the direct proportionality to a , and it vanishes exactly for $a = 0$.

In order to show the impact of a on WW couplings in more detail we provide the same computation in Fig. 5 imposing $a = 0$ by hand for the fit with $\sin \theta = 0.1$ (the most illustrative case). The difference between this and the top panel of Fig. 4 is only noticeable for $R/g_5^2 \lesssim 0.5$; and now the saturation is reached sooner. At the major part of the R/g_5^2 axis the scale of $SO(5)$ breaking is of little consequence for the couplings discussed. The importance of the S constraint at very small values of R/g_5^2 is doubtful. At the same time, this area turns out relevant if we assume that the CH value is close to the QCD one, or if we take into account the estimations of these couplings made in other studies.

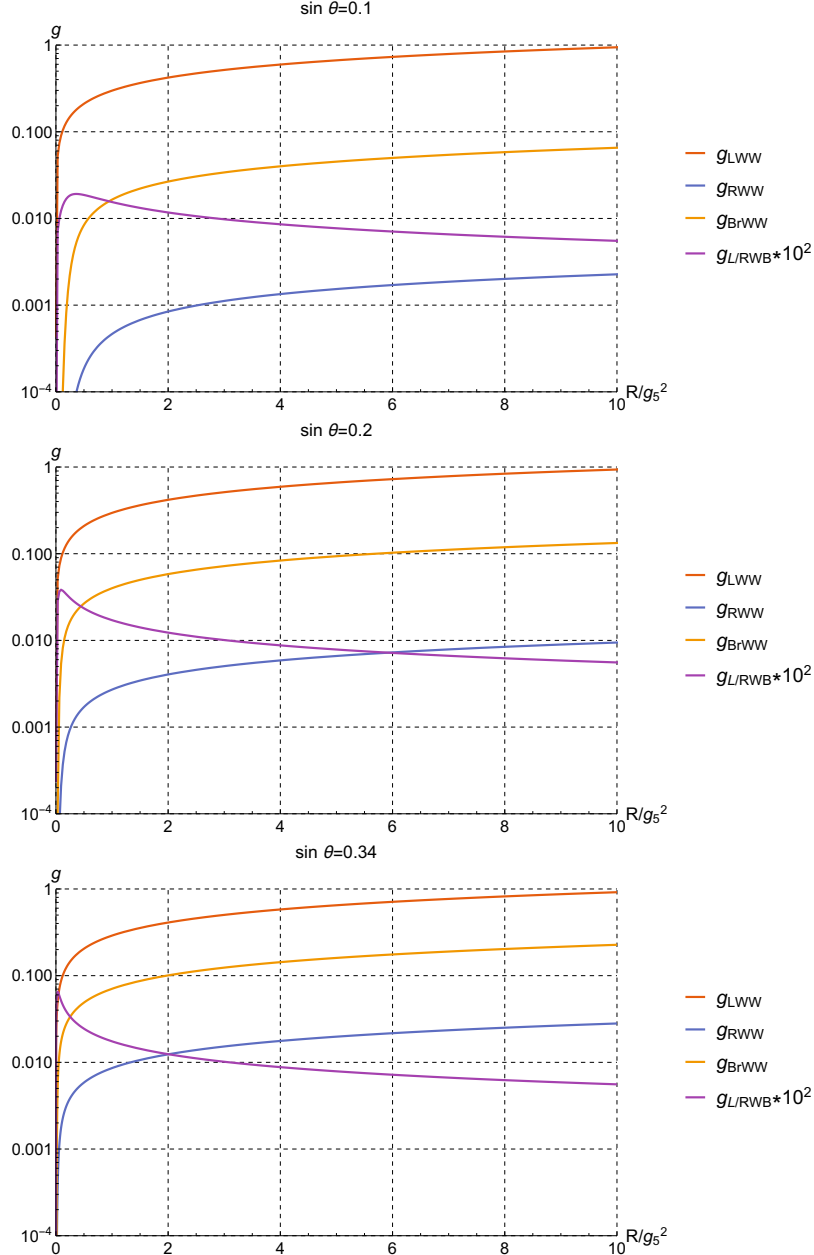


FIG. 4. Couplings of the left, right and broken composite resonances to the W^+W^- and $W^\pm B$ pairs.

It is not easy to make comparison between the values of the couplings obtained here and possible experimental bounds because in the analyses of the LHC experimental data on resonances decaying into WW or WZ pairs some benchmark signal models are normally used (Kaluza–Klein graviton in extra dimension, extended gauge model of W' and Z' , and others). However, in a more model-independent framework of Ref. [37] we find that the characteristic scale for the couplings is of order $0.001 \div 0.010$. g_{LWW} and g_{BrWW} tend to be much larger unless computed at very small R/g_5^2 . We can only speculate about the effect of including quantum corrections in our calculation. Barring large corrections, the comparison with Ref. [37] really indicates lowish values for R/g_5^2 .

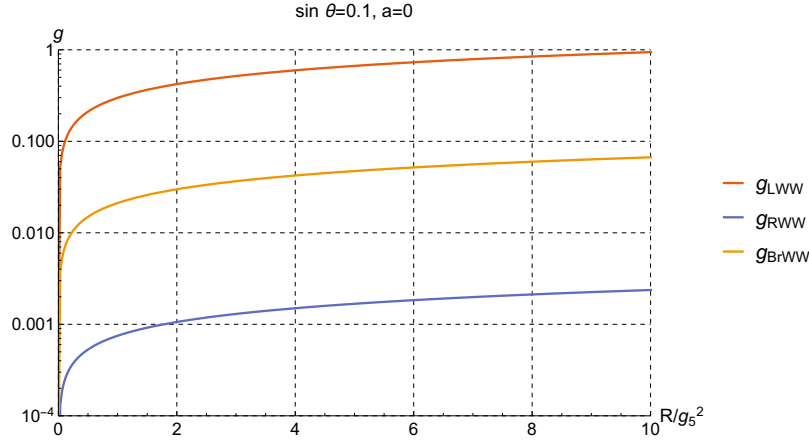


FIG. 5. Example of the couplings estimated for a completely vanishing value of a .

VII. CONCLUSIONS

In this study we used the bottom-up holographic approach to have a fresh look at non-perturbative aspects of CH models with a global breaking pattern $SO(5) \rightarrow SO(4)$ and a gauge group misaligned with the unbroken group. With the purpose of being as close as possible to the characteristics of a confining theory (presumed to be underlying the EWSBS) we chose to work in a 5D SW framework inspired by effective models of QCD and consisting in a generalized sigma model coupled both to the composite resonances and to the SM gauge bosons. The 5D model is similar to that of successful AdS/QCD constructions, specifically to our earlier work [21], and depends on the two ansatz functions: the SW dilaton profile $\Phi(z)$ and the symmetry-breaking $f(z)$. The microscopic nature of the breaking, besides being triggered by some new strong interactions with an hyper-color group, is factored out and every effort have been taken to make predictions as independent of it as possible.

We investigated the dynamics of ten vector (unbroken and broken) and four Goldstone (one of them related to the Higgs) 5D fields. Though for the unbroken vectors the situation is much similar to a generic AdS/QCD model, in the broken sector we have developed a procedure that relates the Goldstone fields to the fifth component A_z^i . That is not just a gauge-Higgs construction because there are as well definite independent Goldstone modes in the bulk. The resulting Goldstone description is quite different from that of the vector fields. The proposed procedure is ratified by the agreement of the hWW and $hhWW$ characteristic couplings to those of the general MCHM. The Higgs remains massless as long as we do not take into account the quantum corrections.

In the paper we lay emphasis on the following issues of phenomenological interest:

- derivation of the spectra of the new states in the broken and unbroken channels;
- connection to the EW sector (masses of the gauge bosons and electroweak precision observables);
- triple couplings of the new heavy resonances to W^+W^- and $W^\pm B$;
- in-depth analysis of the realization of the first and second Weinberg sum rules and the study of their convergence.

The holographic effective theory describes the composite resonances; their maximum number N_{max} is found to be related to the theory natural UV cut-off ε . Adhering to one of these cut-offs is necessary to derive relations involving resonance decay constants and masses. The latter stay cut-off independent as befits physical observables. The only but very significant exception is the “pion decay constant” F . We made a hypothesis that ε can be taken as related to the characteristic range of the CH effective theory, and provided numerical estimations for the value of N_{max} . Moreover, the two Weinberg sum rules hold their validity just in a formal sense as the sum over resonances has to be cut off. The sum rules are logarithmically divergent, and this implies that they are not saturated at all by just the first resonance. We believe it to be a common feature of AdS/CFT models, detached from the particularities of our setup, as it is also present in holographic QCD. We can regard it as a general serious flaw of the bottom-up holographic models, and hence a realistic CH theory could also have the sum rules more similar to those of actual QCD.

The minimal set of input parameters in our model is: $\sin\theta$, a , and $\frac{g_5^2}{R}$. There are constraints coming from the W mass (EW scale), the S parameter and the existing experimental bounds on κ_V ($\sin\theta$). Their consideration allows us to estimate the masses for the composite resonances. It is not difficult to find areas in the parameter space where a resonance between 2 and 3 TeV is easily accommodated. The presented technique offers the possibility of deriving trilinear couplings of a type WW , WB –new composite resonance. They are of interest because the SM gauge boson scattering is regarded as the process for the new vector resonance production in collider experiments.

It is compelling to extend the proposed framework to other non-minimal symmetry breaking patterns, especially the ones that could be supported by a non-exotic theory at the microscopic level. Then, it would be reasonable to include more quantities of physical interest into the analysis.

ACKNOWLEDGMENTS

We acknowledge financial support from the following grants: FPA2016-76005-C2-1-P and PID2019-105614GB-C21 (MICINN), and 2017SGR0929 (Generalitat de Catalunya). A.K. acknowledges the financial support of the fellowship BES-2015-072477. The activities of ICCUB are supported by a Maria de Maeztu grant.

-
- [1] J. Maldacena, *Int. J. Theor. Phys.* **38**, 1113 (1999), arXiv:hep-th/9711200.
 - [2] S. Gubser, I. Klebanov, and A. Polyakov, *Phys. Lett. B* **428**, 105 (1998), arXiv:hep-th/9802109.
 - [3] E. Witten, *Adv. Theor. Math. Phys.* **2**, 253 (1998), arXiv:hep-th/9802150.
 - [4] J. Erlich, E. Katz, D. T. Son, and M. A. Stephanov, *Phys. Rev. Lett.* **95**, 261602 (2005), arXiv:hep-ph/0501128v2.
 - [5] L. Da Rold and A. Pomarol, *Nucl. Phys. B* **721**, 79 (2005), arXiv:hep-ph/0501218.
 - [6] A. Karch, E. Katz, D. T. Son, and M. A. Stephanov, *Phys. Rev. D* **74**, 015005 (2006), arXiv:hep-ph/0602229v2.
 - [7] D. B. Kaplan and H. Georgi, *Phys. Lett. B* **136**, 183 (1984); D. B. Kaplan, H. Georgi, and S. Dimopoulos, *Phys. Lett. B* **136**, 187 (1984); H. Georgi, D. B. Kaplan, and P. Galison,

- Phys. Lett. B **143**, 152 (1984); H. Georgi and D. B. Kaplan, Phys. Lett. B **145**, 216 (1984); M. J. Dugan, H. Georgi, and D. B. Kaplan, Nucl. Phys. B **254**, 299 (1985).
- [8] K. Agashe, R. Contino, and A. Pomarol, Nucl. Phys. B **719**, 165 (2005), arXiv:hep-ph/0412089.
- [9] K. Agashe and R. Contino, Nucl. Phys. B **742**, 59 (2006), arXiv:hep-ph/0510164.
- [10] A. D. Medina, N. R. Shah, and C. E. Wagner, Phys. Rev. D **76**, 095010 (2007), arXiv:0706.1281 [hep-ph].
- [11] R. Contino, Y. Nomura, and A. Pomarol, Nucl. Phys. B **671**, 148 (2003), arXiv:hep-ph/0306259v1.
- [12] G. Panico, M. Serone, and A. Wulzer, Nucl. Phys. B **739**, 186 (2006), arXiv:hep-ph/0510373.
- [13] M. Serone, New J. Phys. **12**, 075013 (2010), arXiv:0909.5619 [hep-ph].
- [14] G. Panico, M. Safari, and M. Serone, JHEP **02**, 103 (2011), arXiv:1012.2875 [hep-ph].
- [15] Y. Hosotani, Phys. Lett. B **126**, 309 (1983).
- [16] A. Falkowski and M. Perez-Victoria, JHEP **2008**, 107 (2008), arXiv:0806.1737 [hep-ph].
- [17] S. Gashorowicz and D. A. Geffen, Rev. Mod. Phys. **41**, 531 (1969); A. H. Fariborz, R. Jora, and J. Schechter, Phys. Rev. D **72**, 034001 (2005); D. Parganlija, F. Giacosa, and D. H. Rischke, Phys. Rev. D **82**, 054024 (2010), arXiv:1003.4934 [hep-ph].
- [18] J. Hirn and V. Sanz, JHEP **2005**, 030 (2005), arXiv:hep-ph/0507049.
- [19] J. Hirn, N. Rius, and V. Sanz, Phys. Rev. D **73**, 085005 (2006), arXiv:hep-ph/0512240v2.
- [20] L. Cappiello, G. D'Ambrosio, and D. Greynat, Eur. Phys. J. C **75**, 465 (2015), arXiv:1505.01000 [hep-ph].
- [21] D. Espriu and A. Katanaeva, Phys. Rev. D **101** (2020), arXiv:2001.08723 [hep-ph].
- [22] B. Bellazzini, C. Csáki, and J. Serra, Eur. Phys. J. C **74**, 2766 (2014), arXiv:1401.2457 [hep-ph].
- [23] G. Panico and A. Wulzer, Lect. Notes Phys. (2016), arXiv:1506.01961v2 [hep-ph].
- [24] G. Ferretti and D. Karateev, JHEP **03**, 077 (2014), arXiv:1312.5330 [hep-ph].
- [25] G. Cacciapaglia and F. Sannino, JHEP **04**, 111 (2014), arXiv:1402.0233 [hep-ph].
- [26] O. Aharony, S. S. Gubser, J. M. Maldacena, H. Ooguri, and Y. Oz, Phys. Rept. **323**, 183 (2000), arXiv:hep-th/9905111 [hep-th].
- [27] D. Z. Freedman, S. D. Mathur, A. Matusis, and L. Rastelli, Nucl. Phys. B **546**, 96 (1999), arXiv:hep-th/9804058.
- [28] L. Reinders, H. Rubinstein, and S. Yazaki, Phys. Rep. **127**, 1 (1985).
- [29] S. S. Afonin and D. Espriu, JHEP **2006**, 047 (2006), arXiv:hep-ph/0602219.
- [30] G. Altarelli and R. Barbieri, Phys. Lett. B **253**, 161 (1991).
- [31] M. E. Peskin and T. Takeuchi, Phys. Rev. D **46**, 381 (1992).
- [32] S. Weinberg, Phys. Rev. Lett. **18**, 507 (1967).
- [33] P. A. Zyla *et al.* (Particle Data Group), Prog. Theor. Exp. Phys. **2020**, 083C01 (2020).
- [34] G. Aad *et al.* (The ATLAS collaboration), JHEP **2015**, 206 (2015), arXiv:1509.00672v2 [hep-ex].
- [35] G. Aad *et al.* (ATLAS), Phys. Rev. D **101**, 012002 (2020), arXiv:1909.02845 [hep-ex].
- [36] A. M. Sirunyan *et al.* (CMS), Eur. Phys. J. C **79**, 421 (2019), arXiv:1809.10733 [hep-ex].
- [37] R. Delgado, A. Dobado, D. Espriu, C. Garcia-Garcia, M. Herrero, X. Marcano, and J. Sanz-Cillero, JHEP **11**, 098 (2017), arXiv:1707.04580 [hep-ph].
- [38] A. Erdélyi, ed., *Higher transcendental functions (Bateman Manuscript Project)*, Vol. 1 (McGraw-Hill, New York, 1953).

Appendix A: Confluent hypergeometric equation and its solutions

The confluent hypergeometric equation is given as

$$y\varphi''(y) + (c - y)\varphi'(y) - a\varphi(y) = 0. \quad (\text{A1})$$

The values of parameters a and c define the types of solution one would get [38]. We abstain from considering solutions whose IR asymptotics tend to explode.

For the positive integer values $c = 1, 2, 3, \dots$ we have

$$\varphi(y) = C_1 {}_1F_1(a, c; y) + C_2 \Psi(a, c; y), \quad (\text{A2})$$

where ${}_1F_1(a, c; y)$ is called the Kummer function and $\Psi(a, c; y)$ is the Tricomi function.

However, in the paper we frequently meet the cases of non-positive integer c . ${}_1F_1(a, c; y)$ has poles at $c = 0, -1, -2, \dots$, while the Tricomi function can generally be analytically continued to any integer value of c . In that situation we can choose another two solutions from the fundamental system of solutions:

$$\varphi(y) = C_1 y^{1-c} {}_1F_1(a - c + 1, 2 - c; y) + C_2 \Psi(a, c; y). \quad (\text{A3})$$

Let us discuss several properties of these confluent hypergeometric functions [38]:

- The Tricomi functions with different arguments are related via

$$\Psi(a, c; y) = y^{1-c} \Psi(a - c + 1, 2 - c; y). \quad (\text{A4})$$

- The Tricomi function exhibits a logarithmic behavior for all integer values of c . Specifically, for the case $c = 1 - n$, $n = 0, 1, 2, \dots$ one has

$$\begin{aligned} \Psi(a, 1 - n; y) = & \frac{(n - 1)!}{\Gamma(a + n)} \sum_{r=0}^{n-1} \frac{(a)_r y^r}{(1 - n)_r r!} + \frac{(-1)^{n-1}}{n! \Gamma(a)} \left({}_1F_1(a + n, n + 1; x) y^n \ln y + \right. \\ & \left. + \sum_{r=0}^{\infty} \frac{(a + n)_r}{(n + 1)_r} [\psi(a + n + r) - \psi(1 + r) - \psi(1 + n + r)] \frac{y^{n+r}}{r!} \right), \end{aligned} \quad (\text{A5})$$

here the Pochhammer symbol is $(a)_n = 1 \cdot a \cdot (a + 1) \dots (a + n - 1) = \Gamma(a + n) / \Gamma(a)$, $\psi(a)$ is the digamma function; and the first sum is absent for the case $n = 0$.

- The Tricomi function has an infinite sum representation involving the generalized Laguerre polynomials

$$\Gamma(a) \Psi(a, 1 + m; y) = \sum_{n=0}^{\infty} \frac{L_n^m(y)}{n + a}. \quad (\text{A6})$$

- The Kummer function is a (finite) series solution ${}_1F_1(a, c; y) = \sum_{n=0}^{\infty} \frac{(a)_n y^n}{(c)_n n!}$, that has a natural connection with the generalized Laguerre polynomials (for integer $n > 0$, $m > 0$)

$$L_n^m(y) = \frac{(m + 1)_n}{n!} {}_1F_1(-n, m + 1, y). \quad (\text{A7})$$

Appendix B: Derivation of the EOM in the broken sector with $\xi = 1$

Let us assume $A_z^i = \frac{\partial_z \pi^i}{\chi_\pi}$ directly in Eqns. (31)-(33). Then, the system on A_μ^i and π^i simplifies to

$$\begin{aligned} \partial_z \frac{e^{-\Phi(z)}}{z} \partial_z A_\mu^i - \frac{e^{-\Phi(z)}}{z} \square A_\mu^i - \frac{2g_5^2 f^2(z) R^2 e^{-\Phi(z)}}{k_s z^3} A_\mu^i \\ - \partial_\mu \left(\partial_z \frac{e^{-\Phi(z)}}{z} \partial_z \frac{\pi^i}{\chi_\pi} - \frac{2g_5^2 f^2(z) R^2 e^{-\Phi(z)}}{k_s z^3} \frac{\pi^i}{\chi_\pi} \right) = 0 \end{aligned} \quad (\text{B1})$$

$$\partial^\mu A_\mu^i = \square \frac{\pi^i}{\chi_\pi} \quad (\text{B2})$$

The condition of Eqn. (34) holds, and together with Eqn. (B2) it implies that

$$\square^2 \frac{\pi^i}{\chi_\pi} = 0. \quad (\text{B3})$$

With the use of the identity $A_\mu^{i||} = \frac{\partial_\mu \partial^\nu}{\square} A_\nu^i = \partial_\mu \frac{\pi^i}{\chi_\pi}$, the longitudinal part in Eqn. (B1) transforms into

$$\begin{aligned} \partial_z \frac{e^{-\Phi(z)}}{z} \partial_z A_\mu^{i||} - \frac{2g_5^2 f^2(z) R^2 e^{-\Phi(z)}}{k_s z^3} A_\mu^{i||} \\ - \partial_\mu \left(\partial_z \frac{e^{-\Phi(z)}}{z} \partial_z \frac{\pi^i}{\chi_\pi} + \frac{e^{-\Phi(z)}}{z} \square \frac{\pi^i}{\chi_\pi} - \frac{2g_5^2 f^2(z) R^2 e^{-\Phi(z)}}{k_s z^3} \frac{\pi^i}{\chi_\pi} \right) = 0. \end{aligned} \quad (\text{B4})$$

All things considered, one of the possible solutions is this set of simultaneously fulfilled equations

$$\partial_z \frac{e^{-\Phi(z)}}{z} \partial_z A_\mu^{i||} - \frac{2g_5^2 f^2(z) R^2 e^{-\Phi(z)}}{k_s z^3} A_\mu^{i||} = 0, \quad (\text{B5})$$

$$\partial_z \frac{e^{-\Phi(z)}}{z} \partial_z \frac{\pi^i}{\chi_\pi} - \frac{2g_5^2 f^2(z) R^2 e^{-\Phi(z)}}{k_s z^3} \frac{\pi^i}{\chi_\pi} = 0, \quad (\text{B6})$$

$$\square \frac{\pi^i}{\chi_\pi} = 0, \quad (\text{B7})$$

while the transverse mode keeps being described by Eqn. (38).

With this exercise we intend to be reassured that the masslessness of the Goldstones agrees with EOMs (37), (38) and (39) given in the main body of the paper.

Appendix C: Large Q^2 expansion of the correlator Π_{LR}

Here we perform the large Q^2 expansion of Π_{LR} given by

$$\begin{aligned} g_V^2 \Pi_{LR}(Q^2) = \frac{R}{2g_5^2} Q^2 \sin^2 \theta \left\{ \psi \left(1 + \frac{Q^2}{4\kappa^2} \right) - \psi \left(1 + \frac{Q^2}{4\kappa^2} + a \right) \right. \\ \left. - \frac{4\kappa^2}{Q^2} a \left[\ln \kappa^2 \varepsilon^2 + 2\gamma_E + \psi \left(1 + \frac{Q^2}{4\kappa^2} + a \right) \right] \right\}, \end{aligned} \quad (\text{C1})$$

by means of using the infinite series representation of the digamma function. From the series representation of the Γ -function it could be derived [38] that

$$\psi(1+z) = -\gamma_E + \sum_{n=1}^{\infty} \frac{z}{n(n+z)}, \quad (\text{C2})$$

and that is valid for $z \neq -1, -2, \dots$. For the particular ψ 's of Eqn. (C1) we have

$$\lim_{Q^2 \rightarrow \infty} \psi \left(\frac{Q^2}{4\kappa^2} + 1 \right) = -\gamma_E + \sum_{n=0}^{\infty} \frac{1}{n+1} \sum_{k=0}^{\infty} \left(\frac{-M_V^2(n)}{Q^2} \right)^k, \quad (\text{C3})$$

$$\lim_{Q^2 \rightarrow \infty} \psi \left(\frac{Q^2}{4\kappa^2} + 1 + \frac{(g_5 R f)^2}{2k_s} \right) = -\gamma_E + \left(1 + \frac{2\kappa^2 (g_5 R f)^2}{k_s Q^2} \right) \sum_{n=0}^{\infty} \frac{1}{n+1} \sum_{k=0}^{\infty} \left(\frac{-M_A^2(n)}{Q^2} \right)^k,$$

where for $k=0$ we have $\lim_{N \rightarrow \infty} \sum_{n=1}^N \frac{1}{n} = \ln N + \gamma_E + \mathcal{O}(1/N)$.

Substitution of the series expansions yields order by order for $g_V^2 \Pi_{LR}(Q^2)/Q^2$

$$\left(\frac{1}{Q^2} \right)^0 : \quad \sin^2 \theta \frac{R}{2g_5^2} \left(\sum_{n=0}^{\infty} \frac{1}{n+1} - \sum_{n=0}^{\infty} \frac{1}{n+1} \right); \quad (\text{C4})$$

$$\left(\frac{1}{Q^2} \right)^1 : \quad 4\kappa^2 \sin^2 \theta \frac{R}{2g_5^2} \sum_{n=0}^{\infty} (1-1) - \sin^2 \theta \kappa^2 a \frac{2R}{g_5^2} \left(\ln \varepsilon^2 \kappa^2 + \gamma_E + \sum_{n=0}^{\infty} \frac{1}{n+1} \right); \quad (\text{C5})$$

$$\left(\frac{1}{Q^2} \right)^2 : \quad 4\kappa^4 \sin^2 \theta a \frac{2R}{g_5^2} \sum_{n=0}^{\infty} (1-1). \quad (\text{C6})$$

Considering that 1 and -1 , as well as the fractions in the difference between harmonic sums, appear together for any fixed n we can set these terms to zeros (certainly 0 for a finite sum). The remaining at $1/Q^2$ order parentheses cancel due to Eqn. (63) when the infinite sum is replaced with the one up to N_{max} . Thus, we show that the terms $1/Q^2$ and $1/Q^4$ are absent as long as $N_{max} < \infty$.

Appendix D: Calculations related to the couplings of Higgs to EW bosons

We can factorize the misalignment in Eqns. (98) and (99), and come to the following equation

$$\mathcal{L}_{eff} \supset \frac{g^2 \sin 2\theta}{g_V^2 8\sqrt{2}} h(q) W_\mu^\alpha(k_1) W_\nu^\beta(k_2) \left[\frac{\delta^2 S_{5D}^{(3)}}{\delta\phi_{L\mu}^\alpha(k_1) \delta\phi_{br\nu}^\beta(k_2) h(q)} + \frac{\delta^2 S_{5D}^{(3)}}{\delta\phi_{br\mu}^\alpha(k_1) \delta\phi_{L\nu}^\beta(k_2) h(q)} \right] \quad (\text{D1})$$

$$+ \frac{g^2}{4g_V^2} h(q_1) h(q_2) W_\mu^\alpha(k_1) W_\nu^\beta(k_2) \left[\cos^2 \theta \frac{\delta^2 S_{5D}^{(4)}}{\delta\phi_{L\mu}^\alpha(k_1) \delta\phi_{L\nu}^\beta(k_2) h(q_1) h(q_2)} \right] \quad (\text{D2})$$

$$+ \frac{\sin^2 \theta}{2} \frac{\delta^2 S_{5D}^{(4)}}{\delta\phi_{br\mu}^\alpha(k_1) \delta\phi_{br\nu}^\beta(k_2) h(q_1) h(q_2)} \Big]. \quad (\text{D3})$$

We have made use of the symmetry of the Lagrangian permitting to substitute $\langle h|\mathcal{O}_{L\ \mu}^\alpha\mathcal{O}_{br\ \nu}^\beta|0\rangle = -\langle h|\mathcal{O}_{R\ \mu}^\alpha\mathcal{O}_{br\ \nu}^\beta|0\rangle$ and $\langle hh|\mathcal{O}_{L\ \mu}^\alpha\mathcal{O}_{L\ \nu}^\beta|0\rangle = \langle hh|\mathcal{O}_{R\ \mu}^\alpha\mathcal{O}_{R\ \nu}^\beta|0\rangle = -\langle hh|\mathcal{O}_{L\ \mu}^\alpha\mathcal{O}_{R\ \nu}^\beta|0\rangle$.

Let us explore the triple coupling first. The 5D action provides two types of contributions

$$\frac{\delta^2 S_{5D}^{(3)}}{\delta\phi_{L\mu}^\alpha(k_1)\delta\phi_{br\nu}^\beta(k_2)h(q)} = \delta^{\alpha\beta}\eta_{\mu\nu}\frac{R}{g_5^2}\left(a\kappa^2\int dy\frac{e^{-y}}{y}\pi(y)/\chi_\pi V(k_1,y)A(k_2,y) + \frac{1}{4}\int dy\frac{e^{-y}}{y}\partial_z\pi(y)/\chi_\pi V(k_1,y)\partial_zA(k_2,y)\right), \quad (\text{D4})$$

and the second variation in (D1) evaluates the same but for exchange $k_1 \leftrightarrow k_2$.

Further, we would like to integrate analytically over y . As we substitute the Goldstone profile and the longitudinal vector propagators, all dependence on momenta disappears and the calculation can be performed. For the transverse modes we put the propagators on-shell with $k_1^2 = k_2^2 = M_W^2$ and consider the limit $M_W^2 \ll 4\kappa^2$. Indeed, we naturally expect the composite resonances to have rather large masses and that limit is substantiated numerically in Section VI. Essentially, we set $k_1^2 = k_2^2 = 0$, and the outcoming integral is analogous to the expression with the longitudinal propagators.

In the calculation it is convenient to use the definitions in terms of the resonance sums

$$A(0,z) = F\pi(z)/\chi_\pi = \Gamma(1+a)\Psi(a,0;\kappa^2z^2) = \sum_n \frac{\kappa^2z^2L_n^1(\kappa^2z^2)}{n+1+a},$$

$$\partial_zA(0,z) = F\partial_z\pi(z)/\chi_\pi = 2\kappa^2z(-a)\Gamma(1+a)\Psi(a+1,1;\kappa^2z^2) = -2\kappa^2za\sum_n \frac{L_n(\kappa^2z^2)}{n+1+a}.$$

Then, the variation (D4) could be estimated quite easily due to the orthogonality of the Laguerre polynomials

$$\kappa^2aF^{-1}\frac{R}{g_5^2}\sum_{n_1,n_2}\frac{\int dye^{-y}yL_{n_1}^1(y)L_{n_2}^1(y) + a\int dye^{-y}L_{n_1}(y)L_{n_2}(y)}{(n_1+a+1)(n_2+a+1)} \quad (\text{D5})$$

$$= \frac{1}{2F}\frac{2R\kappa^2a}{g_5^2}\sum_{n_1,n_2}\delta_{n_1n_2}\frac{n_1+1+a}{(n_1+a+1)(n_2+a+1)} = \frac{F}{2}. \quad (\text{D6})$$

Here we used for F^2 the definition of Eqn. (68).

We follow the same lines for the quartic couplings. Let us start with the variation in (D2):

$$\frac{\delta^2 S_{5D}^{(4)}}{\delta\phi_{L\mu}^\alpha(k_1)\delta\phi_{L\nu}^\beta(k_2)h(q_1)h(q_2)} = 2\delta^{\alpha\beta}\eta_{\mu\nu}\frac{R}{4g_5^2}\left(a\kappa^2\int dy\frac{e^{-y}}{y}(\pi(y)/\chi_\pi)^2V(k_1,y)V(k_2,y) \quad (\text{D7})\right.$$

$$\left. + \frac{1}{4}\int dy\frac{e^{-y}}{y}(\partial_z\pi(y)/\chi_\pi)^2V(k_1,y)V(k_2,y)\right)$$

$$= \frac{1}{4}\delta^{\alpha\beta}\eta_{\mu\nu}F^{-2}\frac{2R}{g_5^2}a\kappa^2\sum_n \frac{n+1+a}{(n+1+a)^2} = \frac{1}{4}\delta^{\alpha\beta}\eta_{\mu\nu}. \quad (\text{D8})$$

Unfortunately, the situation becomes more involved with the variation over the broken sources in (D3) because the integrals there are quartic in Laguerre polynomials

$$\begin{aligned} \frac{\delta^2 S_{5D}^{(4)}}{\delta\phi_{br\mu}^\alpha(k_1)\delta\phi_{br\nu}^\beta(k_2)h(q_1)h(q_2)} &= \delta^{\alpha\beta}\eta_{\mu\nu}F^{-2}\frac{R}{g_5^2}a\kappa^2 \\ &\times \sum_{n_1, n_2} \frac{\int dy e^{-y} A^2(0, y) [a/2L_{n_1}(y)L_{n_2}(y) - yL_{n_1}^1(y)L_{n_2}^1(y)]}{(n_1 + a + 1)(n_2 + a + 1)} \end{aligned} \quad (\text{D9})$$

We can make a calculation at $a = 0$, with the result $\frac{\delta^2 S_{5D}^{(4)}}{\delta\phi_{br\mu}^\alpha(k_1)\delta\phi_{br\nu}^\beta(k_2)h(q_1)h(q_2)} = -\frac{1}{2}\delta^{\alpha\beta}\eta_{\mu\nu}$. We extrapolate this estimation to the case of general a when we present the quartic coupling in the effective Lagrangian.

Appendix E: Calculations related to the couplings of vector resonances to EW bosons

Here we calculate the relevant three-point functions first. Diagrammatically, we obtain a vertex and three propagators with their residues attached to it. In the body of the paper we report the effective vertex proceeding from connecting two legs to the physical sources and reducing the third one via putting an n -th resonance on-shell.

There are not that many types of different three-point functions that can be extracted from Eqn. (106)

$$\langle \mathcal{O}_{L\mu_1}^\alpha(q_1)\mathcal{O}_{L\mu_2}^\beta(q_2)\mathcal{O}_{L\mu_3}^\gamma(q_3) \rangle = \langle \mathcal{O}_{R\mu_1}^\alpha(q_1)\mathcal{O}_{R\mu_2}^\beta(q_2)\mathcal{O}_{R\mu_3}^\gamma(q_3) \rangle \quad (\text{E1})$$

$$\begin{aligned} &= i\varepsilon^{\alpha\beta\gamma}\text{Lor}_{\mu_1\mu_2\mu_3}\delta(q_1 + q_2 + q_3)T_{3V}(q_1, q_2, q_3); \\ \langle \mathcal{O}_{L\mu_1}^\alpha(q_1)\mathcal{O}_{br\mu_2}^\beta(q_2)\mathcal{O}_{br\mu_3}^\gamma(q_3) \rangle &= \langle \mathcal{O}_{R\mu_1}^\alpha(q_1)\mathcal{O}_{br\mu_2}^\beta(q_2)\mathcal{O}_{br\mu_3}^\gamma(q_3) \rangle \quad (\text{E2}) \\ &= i\varepsilon^{\alpha\beta\gamma}\text{Lor}_{\mu_1\mu_2\mu_3}\delta(q_1 + q_2 + q_3)\frac{1}{2}T_{V2A}(q_1, q_2, q_3); \end{aligned}$$

$$\begin{aligned} \langle \mathcal{O}_{br\mu_1}^4(q_1)\mathcal{O}_{br\mu_2}^\alpha(q_2)\mathcal{O}_{R\mu_3}^\beta(q_3) \rangle &= -\langle \mathcal{O}_{br\mu_1}^4(q_1)\mathcal{O}_{br\mu_2}^\alpha(q_2)\mathcal{O}_{L\mu_3}^\beta(q_3) \rangle \quad (\text{E3}) \\ &= i\delta^{\alpha\beta}\text{Lor}_{\mu_1\mu_2\mu_3}\delta(q_1 + q_2 + q_3)\frac{1}{2}T_{V2A}(q_3, q_1, q_2). \end{aligned}$$

There, the Lorentz structure of the correlators is collected into

$$\text{Lor}_{\mu_1\mu_2\mu_3}(q_1, q_2, q_3) = \eta_{\mu_1\mu_2}(q_1 - q_2)_{\mu_3} + \eta_{\mu_1\mu_3}(q_3 - q_1)_{\mu_2} + \eta_{\mu_2\mu_3}(q_2 - q_3)_{\mu_1},$$

and we defined the form factors as follows

$$T_{3V}(q_1, q_2, q_3) = \frac{R}{g_5^2} \int dz e^{-\kappa^2 z^2} z^{-1} V(q_1, z) V(q_2, z) V(q_3, z), \quad (\text{E4})$$

$$T_{V2A}(q_1, q_2, q_3) = \frac{R}{g_5^2} \int dz e^{-\kappa^2 z^2} z^{-1} V(q_1, z) A(q_2, z) A(q_3, z). \quad (\text{E5})$$

Now, to consider the possible interactions with W and B bosons we write down the relevant three-point functions

$$\begin{aligned} \langle \mathcal{O}_{L/R\mu_1}^\alpha(q_1) \tilde{J}_{L\mu_2}^\beta(q_2) \tilde{J}_{L\mu_3}^\gamma(q_3) \rangle &= \frac{g^2}{8g_V^2} i\varepsilon^{\alpha\beta\gamma} \text{Lor}_{\mu_1\mu_2\mu_3}(q_1, q_2, q_3) \delta(q_1 + q_2 + q_3) \\ &\times [(1 \pm \cos \theta)^2 T_{3V}(q_1, q_2, q_3) + \sin^2 \theta T_{V2A}(q_1, q_2, q_3)]; \end{aligned} \quad (\text{E6})$$

$$\begin{aligned} \langle \mathcal{O}_{L/R\mu_1}^\alpha(q_1) \tilde{J}_{L\mu_2}^\beta(q_2) \tilde{J}_{R\mu_3}^3(q_3) \rangle &= \langle \mathcal{O}_{L/R\mu_1}^\alpha(q_1) \tilde{J}_{R\mu_2}^3(q_2) \tilde{J}_{L\mu_3}^\beta(q_3) \rangle \\ &= \frac{gg'}{8g_V^2} i\varepsilon^{\alpha\beta 3} \text{Lor}_{\mu_1\mu_2\mu_3}(q_1, q_2, q_3) \delta(q_1 + q_2 + q_3) \\ &\times [(1 - \cos^2 \theta) T_{3V}(q_1, q_2, q_3) - \sin^2 \theta T_{V2A}(q_1, q_2, q_3)]; \end{aligned} \quad (\text{E7})$$

$$\begin{aligned} \langle \mathcal{O}_{br\mu_1}^\alpha(q_1) \tilde{J}_{L\mu_2}^\beta(q_2) \tilde{J}_{L\mu_3}^\gamma(q_3) \rangle &= -\frac{g^2 \sin \theta}{2g_V^2 \sqrt{2}} i\varepsilon^{\alpha\beta\gamma} \text{Lor}_{\mu_1\mu_2\mu_3}(q_1, q_2, q_3) \delta(q_1 + q_2 + q_3) \\ &\times [T_{V2A}(q_2, q_1, q_3) + T_{V2A}(q_3, q_2, q_1)]; \end{aligned} \quad (\text{E8})$$

$$\begin{aligned} \langle \mathcal{O}_{br\mu_1}^\alpha(q_1) \tilde{J}_{L\mu_2}^\beta(q_2) \tilde{J}_{R\mu_3}^3(q_3) \rangle &= \frac{gg' \sin \theta}{2g_V^2 \sqrt{2}} i\varepsilon^{\alpha\beta 3} \text{Lor}_{\mu_1\mu_2\mu_3}(q_1, q_2, q_3) \delta(q_1 + q_2 + q_3) \\ &\times [T_{V2A}(q_2, q_1, q_3) - T_{V2A}(q_3, q_2, q_1)]; \end{aligned} \quad (\text{E9})$$

$$\begin{aligned} \langle \mathcal{O}_{br\mu_1}^4(q_1) \tilde{J}_{L\mu_2}^\alpha(q_2) \tilde{J}_{L\mu_3}^\beta(q_3) \rangle &= \frac{g^2 \sin 2\theta}{8\sqrt{2}g_V^2} \delta^{\alpha\beta} \text{Lor}_{\mu_1\mu_2\mu_3}(q_1, q_2, q_3) \delta(q_1 + q_2 + q_3) \\ &\times [T_{V2A}(q_3, q_1, q_2) - T_{V2A}(q_2, q_1, q_3)]; \end{aligned} \quad (\text{E10})$$

$$\begin{aligned} \langle \mathcal{O}_{br\mu_1}^4(q_1) \tilde{J}_{R\mu_2}^3(q_2) \tilde{J}_{R\mu_3}^3(q_3) \rangle &= \frac{g'^2 \sin 2\theta}{8\sqrt{2}g_V^2} \text{Lor}_{\mu_1\mu_2\mu_3}(q_1, q_2, q_3) \delta(q_1 + q_2 + q_3) \\ &\times [T_{V2A}(q_3, q_1, q_2) - T_{V2A}(q_2, q_1, q_3)], \end{aligned} \quad (\text{E11})$$

$$\begin{aligned} \langle \mathcal{O}_{br\mu_1}^4(q_1) \tilde{J}_{L\mu_2}^3(q_2) \tilde{J}_{R\mu_3}^3(q_3) \rangle &= \frac{gg' \sin 2\theta}{8\sqrt{2}g_V^2} \text{Lor}_{\mu_1\mu_2\mu_3}(q_1, q_2, q_3) \delta(q_1 + q_2 + q_3) \\ &\times [T_{V2A}(q_3, q_1, q_2) - T_{V2A}(q_2, q_1, q_3)]. \end{aligned} \quad (\text{E12})$$

Only a few BB -resonance interactions are possible due to the epsilon-tensor on the right-hand side of the holographic three-point functions.

Further, we reduce the leg corresponding to q_1 momentum and consider the limit $q_{2,3}^2 \ll 4\kappa^2$ for other two momenta. For the n -th excitation of the left/right resonances in the unbroken sector that means:

$$T_{3V}(q_1, q_2, q_3) \rightarrow \sqrt{\frac{R}{2g_5^2(n+1)}} \int dy e^{-y} L_n^1(y) = \sqrt{\frac{R}{2g_5^2(n+1)}}, \quad (\text{E13})$$

$$T_{V2A}(q_1, q_2, q_3) \rightarrow \sqrt{\frac{R}{2g_5^2(n+1)}} \int dy e^{-y} L_n^1(y) \Gamma^2(1+a) \Psi^2(a, 0; y), \quad (\text{E14})$$

where the latter integral can be calculated for a given n . For $n=0$: $1 - 2a + 2a^2\psi_1(1+a)$.

For the n -th excitation of the resonances from the broken sector one of the broken legs should be reduced, and we get

$$\begin{aligned} T_{V2A}(q_2, q_1, q_3) \text{ or } T_{V2A}(q_3, q_2, q_1) &\rightarrow \sqrt{\frac{R}{2g_5^2(n+1)}} \sum_{n'} \frac{\int dy e^{-y} L_n^1(y) L_{n'}^1(y)}{n' + 1 + a} \\ &= \sqrt{\frac{R(n+1)}{2g_5^2}} \frac{1}{n+1+a}. \end{aligned} \quad (\text{E15})$$

Some triple couplings will not be included in the effective Lagrangian. These are: $A_{br}^4 W^\alpha W^\alpha$, $A_{br}^4 BB$, $A_{br}^4 W^3 B$, $A_{br}^\alpha W^\beta B$. The reason for it is that in the corresponding three-point functions the leading term in the limit $q_{2,3}^2 \ll 4\kappa^2$ is zero due to the subtraction of the form factors. The first contribution is $\sim \frac{M_W^2}{4\kappa^2}$ and, thus, is strongly suppressed. We abstain from considering observables of this order in this work.